

# A comprehensive screening of the whole proteome of hantavirus and designing a multi-epitope subunit vaccine for cross-protection against hantavirus: Structural vaccinology and immunoinformatics study

Faruq Abdulla<sup>a</sup>, Zulkar Nain<sup>b</sup>, Md. Moyazzem Hossain<sup>c</sup>, Shifath Bin Syed<sup>b</sup>, Md Shakil Ahmed Khan<sup>b</sup>, Utpal Kumar Adhikari<sup>d,\*</sup>

<sup>a</sup> Department of Statistics, Faculty of Sciences, Islamic University, Kushtia, 7003, Bangladesh

<sup>b</sup> Department of Biotechnology and Genetic Engineering, Faculty of Biological Sciences, Islamic University, Kushtia, 7003, Bangladesh

<sup>c</sup> Department of Statistics, Faculty of Mathematical & Physical Sciences, Jahangirnagar University, Savar, Dhaka, 1342, Bangladesh

<sup>d</sup> School of Medicine, Western Sydney University, Campbelltown, NSW, 2560, Australia



## ARTICLE INFO

### Keywords:

Orthohantavirus  
Immunoinformatics  
Immune simulation  
Molecular dynamics simulation  
*In silico* cloning  
Cross-protection

## ABSTRACT

Hantaviruses are an emerging zoonotic group of rodent-borne viruses that are having serious implications on global public health due to the increase in outbreaks. Since there is no permanent cure, there is increasing interest in developing a vaccine against the hantavirus. This research aimed to design a robust cross-protective subunit vaccine using a novel immunoinformatics approach. After careful evaluation, the best predicted cytotoxic & helper T-cell and B-cell epitopes from nucleocapsid proteins, glycoproteins, RdRp proteins, and non-structural proteins were considered as potential vaccine candidates. Among the four generated vaccine models with different adjuvant, the model with toll-like receptor-4 (TLR-4) agonist adjuvant was selected because of its high antigenicity, non-allergenicity, and structural quality. The selected model was 654 amino acids long and had a molecular weight of 70.5 kDa, which characterizes the construct as a good antigenic vaccine candidate. The prediction of the conformational B-lymphocyte (CBL) epitope secured its ability to induce the humoral response. Thereafter, disulfide engineering improved vaccine stability. Afterwards, the molecular docking confirmed a good binding affinity of  $-1292 \text{ kJ/mol}$  with considered immune receptor TLR-4 and the dynamics simulation showed high stability of the vaccine-receptor complex. Later, the *in silico* cloning confirmed the better expression of the constructed vaccine protein in *E. coli* K12. Finally, *in silico* immune simulation, significantly high levels of immunoglobulin M (IgM), immunoglobulin G1 (IgG1), cytotoxic & helper T lymphocyte (CTL & HTL) populations, and numerous cytokines such as interferon- $\gamma$  (IFN- $\gamma$ ), interleukin-2 (IL-2) etc. were found as coherence with actual immune response and also showed faster antigen clearance for repeated exposures. Nonetheless, experimental validation can demonstrate the safety and cross-protective ability of the proposed vaccine to fight against hantavirus infection.

## 1. Introduction

The hantaviruses are emerging as they cause about 150,000–200,000 outbreaks in humans annually with case fatality rates of 0.1%–50% depending on the species with the majority occurring in Asia [1–4]; and their amplitude and magnitude of outbreaks are increasing day by day. The hantaviruses are negative-stranded and trisegmented zoonotic viruses hosted by rodents, shrews, moles, bats, and insects [5,6]. Its genome composed of three RNA molecules such as small (S) encodes nucleoprotein (N), medium (M) encodes glycoproteins (Gn and Gc), and

large (L) encodes RNA-dependent RNA polymerase (RdRp) or L protein [7]. Hantaviruses can occur two human acute febrile diseases so-called hemorrhagic fever with renal syndrome (HFRS) in the old world and hantavirus cardiopulmonary syndrome (HCPS) in the new world [8]. Although the hantaviruses in both world have similarity in their nucleotide sequence, they induce different diseases [9]. A report published on 24<sup>th</sup> March 2020 by Anadolu Agency, where it is reported that the hantaviruses transmitted from rodents to humans and man died of hantavirus infection with fatigue & muscle aches symptoms [10]. China classified the HFRS as a class B notifiable disease for its severity [11–13]

\* Corresponding author.

E-mail addresses: [uk.adhikari@hotmail.com](mailto:uk.adhikari@hotmail.com), [u.adhikari@westernsydney.edu.au](mailto:u.adhikari@westernsydney.edu.au) (U.K. Adhikari).

with an aggregate of 112,177 cases and 1116 deaths over the past decade [14,15]. From 1978 to 1995, 3145 HFRS cases with morbidity of 1.7% were reported in Asian Russia [16] and in Korea, annually 300–500 cases are recorded with 1% mean fatality [1]. Also, Europe diagnosed annually over 3000 HFRS cases [1] and over 2800 cases were recorded in Latvia [17]. There is an important HFRS case has been recorded in Ecuador [18]. Furthermore, HFRS cases were reported in Vietnam, Singapore, Thailand, India, Sri Lanka, Finland, Sweden, France, Germany, Balkans, Czech Republic, Switzerland, Poland, Greece, Lithuania, Estonia, Slovenia, Turkey, United Kingdom, and all about the African countries [1]. In contrast, the United States reported 624 HCPS cases between the period 1993 to 2013 [1] and since 1995, HCPS listed as a notifiable disease since 1995 [19]. In Chile, 837 HCPS cases have been recorded with fatality rate of 36.1% during 2013 and 1600 cases have been reported in Brazil before 2013 [1]. Argentina reported annually 100–200 HCPS cases and some cases occurred in Canada [1]. Furthermore, the serological evidence and cases of HCPS have been identified in Central America and also Bolivia, Colombia, Suriname, French Guiana, Uruguay, Paraguay, Venezuela, and Peru have reported some HCPS cases [1,20–22].

Humans are infected by hantaviruses via excreta, saliva, and urine of the infected animals [8]. The main route of the human infection is the inhalation of aerosols contaminated with virus [8]. The human kidney and lung are the main targeted organs of HFRS-associated and HCPS-associated viruses, respectively [1]. In humans, hantaviruses mainly infect vascular endothelial cells and dysfunctioning them in capillaries and small vessels. Therefore, the dramatic increase in vascular permeability is the basic pathology of hantavirus-associated diseases [13]. Basically, HFRS patients have manifested five clinical phases such as fever, hypotensive shock, oliguric, polyuric, and convalescent and on the other hand, prodromal, cardiopulmonary, and convalescent are the three clinical phases of HCPS patients [1]. The incidence rate of male is greater than females [1]. Acute encephalomyelitis, bleeding, multiorgan dysfunction, pituitary hemorrhage, glomerulonephritis, pulmonary edema, shock, respiratory distress syndrome, disseminated intravascular coagulation, and lethal outcome are the main complications of HFRS and in contrast, renal insufficiency, thrombocytopenia, bleeding, myalgia, headache, nausea, vomiting, diarrhea, shock, and lethal outcome are associated with HCPS [1]. However, against this severely emerging virus, there are few developed inactivated vaccines have been licensed for humans in Korea and China [23].

The immune response plays a central role to prevent any viral infections including hantavirus infection [1,24]. Recently, the multi-epitope vaccine is the best preventive way of tumors or viral infections [24]. Many researchers studied and designed multi-epitope subunit vaccine against various viruses like HIV [25], Dengue virus [26], Hepatitis B virus [27], Hepatitis C virus [28,29], Ebola virus [30], Chikungunya virus [31], Avian influenza A (H7N9) virus [32], Zika virus [33], Classical swine fever virus [34], Nipah virus [35], and Norovirus [36]. Wang *et al.* predicted the T & B-cell epitopes as potential vaccine candidates by studying the S protein of the Severe Acute Respiratory Syndrome Coronavirus 2 (SARS-CoV-2) using computer-based immunoinformatics approach [37] and Kalita *et al.* designed a multi-epitope based peptide vaccine candidate through analyzing the nucleocapsid protein, membrane glycoprotein, and surface spike glycoprotein of the novel coronavirus SARS-CoV-2 by integrated immunoinformatics approach [38]. Like the SARS-CoV-2 and other pandemics & viruses, multi-epitope vaccine could be a novel and potential preventive way against the newly emerging zoonotic virus and probably the future pandemic called hantavirus. An ideal multi-epitope-based vaccine should comprises series of or overlapping epitopes so that its every basic unit called antigenic peptide fragment can elicit both of the cellular & humoral immune response against the targeted tumor or virus [24]. In present, the multi-epitope subunit vaccine approach has fascinated increased global interest over

traditional or single-epitope vaccine as it has a unique design mechanism with some properties [24]: (a) contains multiple major histocompatibility complex (MHC)-restricted epitopes for maximizing population coverage; (b) contains overlapping CTL, HTL, and B-cell epitopes for inducing strong cellular and humoral immune response simultaneously and limiting the peptide length; (c) contains multiple epitopes of various tumor/virus antigens for protecting many strains of targeted tumors or viruses; (d) start with adjuvant for amplifying the immunogenicity and long-lasting immune responses; and (e) reduce unwanted components for avoiding adverse effects. On the other hand, a cross-protective subunit multi-epitope vaccine should contain epitopes that are conserved to many strains of the targeted pathogenic agent [28]. In addition, the vaccine should contain epitopes from the antigen which have the ability to induce cross-protective immune response. The nucleocapsid proteins of hantavirus are considered to be vital antigens of a wide range of reactive vaccines against hantavirus infection because research has shown that these proteins circulating in different continents can provide high cross-protection in animals [39]. Nosrati *et al.* designed a cross-protective multi-epitope vaccine against hepatitis C virus (HCV) using potential T & B-cell epitopes of some segments of E1 and E2 proteins of HCV where the segments were found to be conserved in different serotypes of HCV [28]. However, a designed multi-epitope subunit vaccine will be robust if it respond as a powerful prophylactic and therapeutic agent against many strains of the targeted tumor or virus. This study has applied a chain of immunoinformatics approaches on the whole proteome of hantavirus for developing a robust cross-protective multi-epitope vaccine using the screened robust CTL, HTL, and B-cell vaccine candidates. Furthermore, the developed vaccine was studied for its antigenicity & allergenicity and subsequently the structural prediction was done. Moreover, disulfide engineering, binding affinity with the immune receptor, and the molecular dynamics simulation (MDS) of the best vaccine-receptor docked complex were sequentially studied. In addition, the codon adaptation, *in silico* cloning, and *in silico* immune simulation of the constructed vaccine protein were performed.

## 2. Material and methods

### 2.1. Retrieval of whole proteome, grouping, and assurance of highest antigenic protein of orthohantavirus

To develop a multi-epitope vaccine model with several epitope, the entire proteome of the orthohantavirus was identified and three gene products such as nucleoprotein, envelope glycoprotein (Gn/G1 and Gc/G2) and RdRp protein were found [9]. The complete amino acid sequences of those proteins were retrieved from the National Institute of Allergy and Infectious Diseases (NIAID) Virus Pathogen Database and Analysis Resource (ViPR) through the web site at [www.viprbrc.org](http://www.viprbrc.org). The retrieved protein sequences were then grouped according to their strain, protein category, and epidemic nature. Thereafter, the protein sequences of the targeted groups (classified causative organisms of HFRS and HCPS) were submitted as input in the VaxiJen v2.0 server [40] available at <http://www.ddg-pharmfac.net/vaxijen/VaxiJen/VaxiJen.html> for predicting their antigenicity and ensuring the highest antigenic proteins for the final dataset preparation, where the threshold parameter was fixed as default.

### 2.2. Prediction of T & B-cell epitopes and major histocompatibility complex (MHC) alleles

The cytotoxic T-cells are essential for immune defense against intracellular pathogens, including virus, bacteria, and tumor surveillance. Therefore, the highly antigenic proteins were subjected to the NetCTL v1.2 [41] server available at <http://www.cbs.dtu.dk/services/NetCTL/> for predicting 9-mer CTL epitopes. In the NetCTL server, we predicted the epitopes for 12 super types with a combined threshold

score of 0.5. Furthermore, the immune epitope database (IEDB) MHC I Binding tool available at <http://tools.iedb.org/mhci/> was used to predict the MHC-I binding alleles corresponding to each CTL epitopes [42]; where the parameters consensus and human were set as the prediction method and MHC source species, respectively. On the other hand, the helper T-cell epitope prediction is also a key stage of epitope-based vaccine design because helper T-cells provide agnate help for the propagation of the potent humoral and cellular responses by promoting optimal expansion of CTLs and maintaining an effective cytotoxic T-cell [43,44]. The 15-mer HTL epitopes with their respective MHC alleles were determined by the IEDB MHC II Binding tool (<http://tools.iedb.org/mhcii/>) utilizing its consensus prediction method [45]. A consensus percentile rank of  $\leq 2$  was set as a cutting point for allele selection because the binding affinity is inversely related to percentile rank. B-cells can play central role for the adaptive immune system by recognizing and providing long-term protection against infectious pathogens through producing antibodies [46]. Consequently, B-cell epitopes prediction is a potential stage of rational vaccine design. To do this, the highly antigenic protein sequences were submitted as input to the LBtope server (<http://crdd.osdd.net/raghava/lbtope/>) where the parameters: support vector machine (SVM) method, LBtope\_Fixed, 20-mer peptide, and the percent of probability is 60% were selected for B cell epitope prediction [47].

### 2.3. Screening of CTL, HTL, and linear B-Lymphocyte (LBL) epitopes for potential vaccine candidates

The predicted CTL, HTL, and LBL epitopes were screened through antigenicity, allergenicity, toxicity, and conservancy. In addition, maximum population coverage and immunogenicity criterion was used for the T-cell epitope selection. However, immunogenicity also known as the center of the peptide-based vaccine efficacy is the ability of CTL epitopes to trigger humoral and cell-mediated immune response [48]. Consequently, the immunogenicity scores of CTL epitopes were computed through the IEDB MHC I Immunogenicity tool [49] available at <http://tools.iedb.org/immunogenicity/>. The antigenicity of the predicted epitopes were predicted through VaxiJen v2.0 server. The epitope-based vaccine should contain epitopes that are highly conserved between multiple strains or even species for cross-protection against hantavirus [50]. Therefore, the predicted epitopes were submitted to IEDB Conservation Across Antigens tool available at <http://tools.iedb.org/conservancy/> to analyze their conservancy [50]. Another two important characteristics of peptides such as non-allergenicity and non-toxicity were checked using AllerTOP v2.0 [51] and ToxinPred server (<http://crdd.osdd.net/raghava/toxinpred/>) [52], respectively. Finally, the population distribution results of the T-cell epitopes were determined for maximizing population coverage in different ethnic groups by Population Coverage tool [53] (<http://tools.iedb.org/population/>).

### 2.4. Screening of cytokine-inducing HTL epitopes

Several studies exhibited that cytokines have important role in the pathogenesis of human hantavirus infection in both HFRS and HCPS [54–58]. Herein, we predicted the interleukin-10 (IL-10) inducer HTL epitopes through the IL-10Pred server (<https://webs.iiitd.edu.in/raghava/il10pred/>) [59], in which the SVM method and 0.1 cut off value was chosen as selection parameters.

### 2.5. Peptide-allele docking simulation

The predominant binding affinities of the screened epitopes with their respective MHC-restricted human leukocyte antigen (HLA) alleles of the known three-dimensional (3D) structure were evaluated by the molecular docking simulation [60]. Herein, we used PEPFOLD v3.5 server [61] to predict the tertiary structure of the screened epitopes and

the crystal structures of the lowest percentile ranked HLA proteins such as HLA-B\*07:02 (6AT5), HLA-A\*03:01 (2XPG), HLA-A\*11:01 (5WJL), HLA-C\*06:02 (5W6A), HLA-B\*51:01 (1E27), HLA-B\*39:01 (4O2F), HLA-A\*24:02 (4F7M), HLA-B\*40:02 (5IEK), HLA-B\*18:01 (6MT3), & HLA-DRB1\*01:01 (2FSE) [62–71] were retrieved from Protein Data Bank (PDB). The protein and ligand were separated from the complex structure through Discovery Studio v16.0.0.400 and the AutoDock tools were used for the preparation of the protein and ligand files into PDBQT files by selecting the binding region and the number of torsion trees, respectively [72]. Finally, these PDBQT files were analyzed by AutoDockVina software for docking simulation [73].

### 2.6. Clustering of the MHC-Restricted HLA alleles

In vaccine development, the resolved MHC super-families (clusters) play an important role identifying new targets with optimized affinity and selectivity of hits [74]. The MHC HLA proteins with similar binding affinities were well clustered using the structure-based clustering technique [74]. Herein, the MHCcluster v2.0 available at <http://www.cbs.dtu.dk/services/MHCcluster/> was carried out in order to develop the heat map of the functional relationship of the HLAs [75].

### 2.7. Multi-epitope subunit vaccine protein construction

The ideally effective multi-epitope subunit vaccine should be composed of epitopes that can evoke CTL, HTL, and LBL and can trigger effective immune responses against the targeted virus [24]. The screened vaccine candidates were sequentially joined to establish the final vaccine protein. In the vaccine construct, the epitopes were joined by proper linkers for enhancing the immunological response of the vaccine construct and epitope's individual effective function [76]. In this study, the linkers GGGS, GPGPG, and KK were used to intra-connect the CTL, HTL, and LBL epitopes, respectively. Herein, the immunostimulatory adjuvants TLR-4 agonist (RS-09),  $\beta$ 3-defensin,  $\beta$ 3-defensin with RR residues, and 50S ribosomal protein L7/L12 derived from *Mycobacterium tuberculosis* (strain: ATCC 25618/H37Rv) were used as adjuvants to construct four separate vaccine models. The problem of high polymorphic HLA alleles was solved by incorporating the PADRE sequence along with the adjuvants. The adjuvant was fused with the CTL epitope through EAAAK linker. The linkers GGGS, GPGPG, KK, and EAAAK were used in this study because all of these linkers were widely used in previous studies for the design of multi-epitope vaccines [25,26, 77–79]. However, the vaccine protein was started with EAAAK linker and subsequently the adjuvant, EAAAK linker, PADRE sequence, GGGS linker, CTL epitope, GPGPG linker, HTL epitope, KK linker, LBL epitope, KK linker, PADRE sequence added and finally stooped with GGGS linker.

### 2.8. Immunological assessment of the vaccine models

Antigenicity can measure how strongly an antigen binds to the B & T-cell receptor in order to induce the immune response and the formulation of the memory cells [80]. Accordingly, the entire vaccine construct was submitted to the VaxiJen v2.0 server to determine the antigenic nature of the vaccine construct. However, a vaccine should not be allergic as allergic behavior can have serious adverse effects on human life [78]. Therefore, the vaccine construct with two modules, SVM (amino acid composition) and hybrid approach, was analyzed for allergenicity under the AlgPred server (<https://webs.iiitd.edu.in/raghava/algpred/submission.html>) [81]. The allergy score of the vaccine protein was crosscheck by AllerTOP v2.0 and AllergenFP v1.0 servers [82].

### 2.9. Structural prediction of the vaccine models

The whole vaccine constructs were submitted to the Self-Optimized

Prediction Method with Alignment (SOPMA) server ([https://npsa-prabi.ibcp.fr/NPSA/npsa\\_sopma.html](https://npsa-prabi.ibcp.fr/NPSA/npsa_sopma.html)) for predicting the secondary structural features of the vaccine models [83]. As a large portion of the immunoinformatics approach depends on the protein tertiary structure, the three-dimensional (3D) structure prediction is a crucial step for peptide-based vaccine design. Therefore, the 3D structures of the vaccine models were predicted byRaptorX server available at <http://raptox.uchicago.edu/>which is a multiple-template threading based protein structure prediction technique [84].

#### 2.10. Refinement and quality evaluation of the 3D structure of the vaccine construct

Refinement is the crucial technique to determine the better quality structure as the low accuracy limits the further use of the 3D models [85]. The predicted crude 3D model was refined using the GalaxyRefine server (<http://galaxy.seoklab.org/cgi-bin/submit.cgi?type=REFINE>) [86]. The accuracy of the refined 3D model was validated by generating the Ramachandran plot through PROCHECK under the PDBsum server available at [www.ebi.ac.uk/pdbsum/](http://www.ebi.ac.uk/pdbsum/)[87,88]. The refined model also validated by determining the Z-score of the local model quality through the ProSA-web (<https://prosa.services.came.sbg.ac.at/prosa.php>) [89] as well as the non-bonded interactions using ERRAT server (<http://services.mbi.ucla.edu/ERRAT/>) [90].

#### 2.11. Assessment of the vaccine construct for physicochemical properties

We further characterized the vaccine construct by assessing the different physicochemical behaviors such as molecular weight (MW), isoelectric point (pI), estimated half-life, instability index (II), aliphatic index (AI), grand average of hydropathy (GRAVY) value, and solubility. The physicochemical properties (excluding solubility) were computed by analyzing the vaccine protein sequence through the ProtParam tool under the ExPASy (<https://web.expasy.org/protparam/>) [91]. Later, the designed vaccine solubility in *E. coli* was analyzed by the SOLpro tool in the SCRATCH suite [92].

#### 2.12. Mapping of discontinuous B-cell epitopes in designed final vaccine protein

The patch of atoms on the protein surface is termed as the discontinuous or conformational B-lymphocyte (CBL) epitope. It has been predicted that the discontinuous B-cell epitopes will design a molecule that mimics the structure and immunogenic properties of the epitope and can replace it either in the antibody production phase or in the detection of antibodies in medical diagnostics or experimental research [93]. Therefore, the CBL epitopes of the constructed vaccine protein were determined by subjecting the vaccine tertiary structure to the IEDB ElliPro tool available at <http://tools.iedb.org/elliPro/>[93].

#### 2.13. Disulfide engineering of constructed vaccine protein

The increased number of disulfide bonds can increase the protein stability [78]. The Disulfide by Design 2 (DbD2) v2.12 server available at <http://cptweb.cpt.wayne.edu/DbD2/>was carried out to perform the disulfide engineering of designed vaccine structure [94]. The DbD2 can predict the likely residue pairs with the ability to form a disulfide bond by mutating the residues in the pairs with cysteine. Afterwards, the DynaMut server available at <http://biosig.unimelb.edu.au/dynamut/>was then used to check the stability of the designed vaccine protein for the mutation by cysteine of each residue predicted by DbD2 [95]. The DynaMut server predicts the stability based on the vibrational entropy changes, with the positive value indicating a stable protein.

#### 2.14. Vaccine-receptor molecular docking

Molecular docking is a technique for characterizing the ligand molecule at the binding site of the receptor protein by modeling the ligand-receptor complex structure and predicting the preliminary binding parameters of the ligand-receptor complex [96]. After infection, the host's endothelial cells become dysfunctional and pathogenic by the hantavirus [97]. Since the toll-like receptor-4 (TLR-4) can secret several cytokines in the endothelial cells infected by Hantaan virus, it was used as an immunological receptor protein to induce anti-hantavirus immunity [97]. The TLR-4 (PDB ID: 4G8A) was retrieved from Protein Data Bank. The task of molecular docking between vaccine protein & TLR-4 receptor protein was completed by ClusPro 2.0 server available at <http://cluspro.bu.edu/login.php> [98]. The best docked complex would be selected based on the lowest energy score of the complexes. The PatchDock server available at <https://bioinfo3d.cs.tau.ac.il/PatchDock/php.php> [99,100] and the FireDock server available at <http://bioinfo3d.cs.tau.ac.il/FireDock/php.php> [101,102] servers were used to crosscheck the interaction performance of the vaccine construct with the immune receptor TLR-4.

#### 2.15. Molecular dynamics simulation of the best docked vaccine-receptor complex

Molecular dynamic simulation is the most popular computer-aided simulation technique for investigating the physical basis and function of the macromolecular structure [103]. Comparing the essential dynamics of proteins with their normal modes is an alternative powerful tool to the costly atomistic simulation [104–106]. The stability of the vaccine-receptor complex was determined using the iMOD server (iMODS) available at <http://imods.chaconlab.org/>, which analyze the normal modes in internal coordinates and describes the collective functional motions by different measures such as deformability, eigenvalues, and covariance map [107]. The ability of a given molecule to distort at each of its residues is measured by the deformability. The eigenvalue, which relates to each normal mode, indicates the stiffness of motion and is directly related to the energy required to distort the structure. The covariance map represents the coupling between pairs of residues.

#### 2.16. Codon adaptation and in silico cloning of vaccine construct

Codon adaptation can increase the rate of expression of the foreign gene in the host if the codon uses differ from one another in the two organisms. The Java Codon Adaptation Tool (JCat) available at <http://www.jcat.de/>was therefore used to determine the optimized DNA sequence of the designed vaccine protein according to *E. coli* strain K12 [79,108]. The Codon Adaptation Index (CAI) and the percentage of the codon with GC content are the measurement factors for the expression rate. The allowable CAI range and percentage of GC content codon should be 0.8–1.0 and 30–70%, respectively, with the CAI value of 1.0 indicating that the improved DNA sequence is 100% accurate is translated into the vaccine protein [26]. The rho-independent transcription terminators, prokaryotic ribosome binding sites, and cleavage sites of restriction enzymes were avoided by checking three additional options in JCat. In addition, it is ensured that the restriction enzyme cutting sites (XhoI and NdeI) were not present in the optimized DNA sequence. Thereafter, the XhoI and NdeI restriction enzymes were added to the N- and C-terminal sites of the adapted DNA sequence. Lately, the optimized DNA sequence was inserted into the *E. coli* pET28a(+) vector through restriction cloning module of the SnapGene tool to determine the cloned vaccine.

#### 2.17. Immune simulation of vaccine construct

The immune simulation is an important step in understanding the

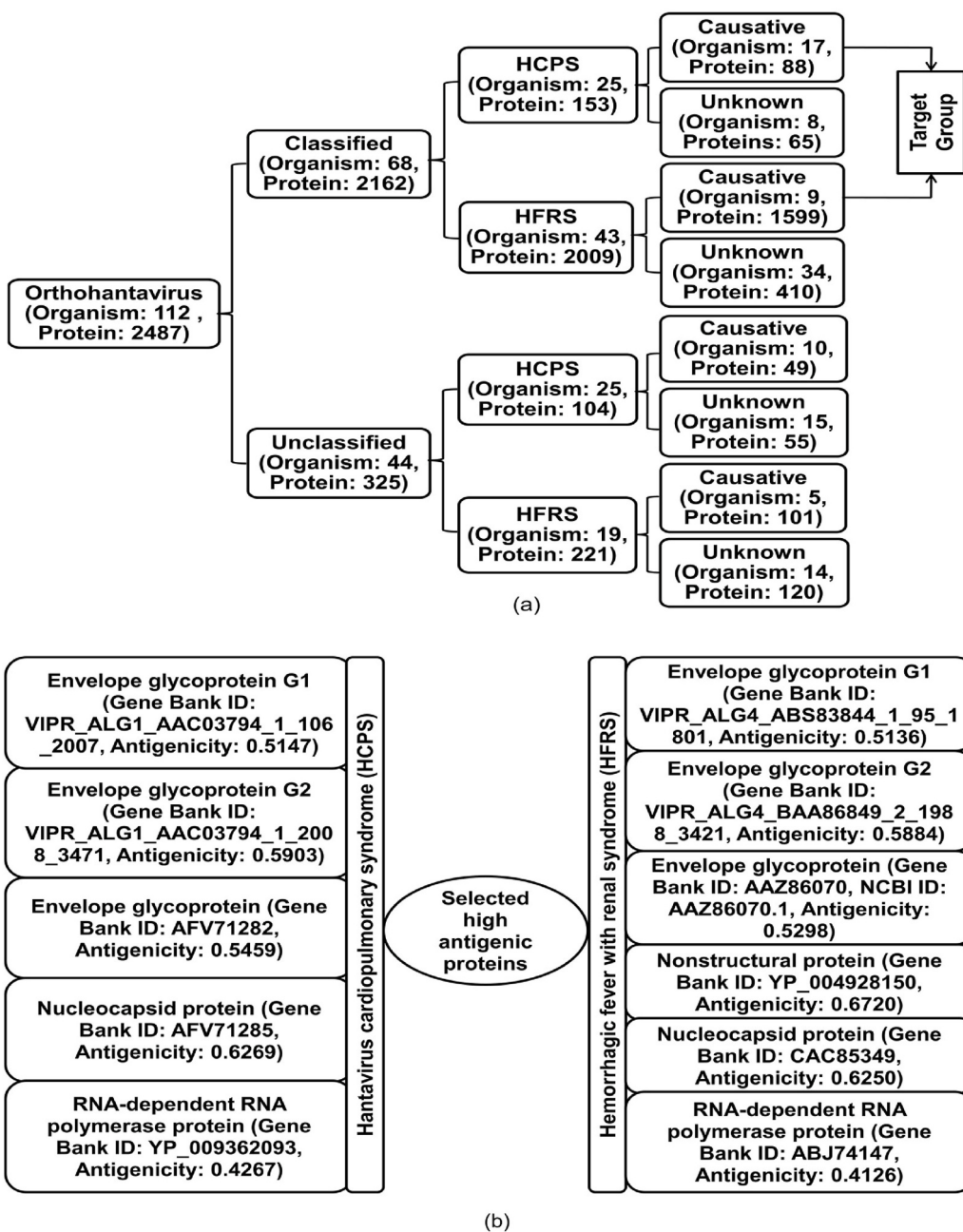


**Fig. 1.** Overview of the analyzed data where (a) indicates the classification of the whole proteome of the Hantavirus retrieved from ViPR database and (b) represents the summary of the highest antigenic proteins.

immune system by determining the immunogenicity and immune response profile of the vaccine protein [109]. The agent-based immune simulator, C-ImmSim available at <http://kraken.iac.rm.cnr.it/C-IMMSIM/> was used to perform the immune simulation of the vaccine construct. The C-ImmSim simulator predicts the immune epitopes and immune interactions using the position-specific scoring matrix (PSSM) and machine learning technique, respectively [109]. The least recommended time interval between doses for most vaccines currently in use is four weeks, and three injections of prophylactic onchocerciasis vaccine are given four weeks apart according to the Onchocerciasis Vaccine for Africa (TOVA) approach [110,111]. Therefore, three injections of the constructed vaccine protein four weeks apart with conserved host HLA alleles and a time step of 1, 84 and 168 were considered (1 time step  $\sim$  8 h of real-life & time step = 1 when injection at time = 0). The simulation volume and simulation steps were set at 110 and 1100, respectively. The

remaining simulation parameters were considered at default (random seed = 12345, what to inject = vaccine (no LPS), adjuvant = 100, and num Ag to inject = 1000). In addition, 12 injections of the engineered peptide sequence with a 4 week dose interval were considered to simulate repeated exposure to the antigen observed in a typical endemic area to look for clonal selection. The degree of diversity referred to as the Simpson index D was interpreted from the illustration.

### 3. Results and discussion

#### 3.1. Representative proteins selection of orthohantavirus

In order to design a candidate multi-epitope vaccine, a total of 2487 protein sequences of 112 organisms of *Orthohantavirus* were retrieved from the NIAID Virus Pathogen Database and Analysis Resource (ViPR)

**Table 1**Potential CD8<sup>+</sup> T-cell vaccine candidates and their characteristics corresponding to each protein of orthohantavirus.

Protein name	Peptide sequence	Start	Combined score	Super type	Antigenicity score	Immunogenicity score	Conservancy for classified-causative group	Conservancy for classified-unknown group	Conservancy for unclassified-causative group	Conservancy for unclassified-unknown group	Toxicity prediction	Allergenicity prediction	# of alleles available in PDB	# of alleles available in not-PDB	Allele
HCPS_GP1	MPITWTGFL	342	1.4992	B7	1.1079	0.4315	100.00% (2/2)	0.00% (0/1)	–	–	Non-Toxin	Non-Allergen	5	9	HLA-B*07:02, HLA-B*53:01, HLA-B*35:01, HLA-B*51:01, HLA-B*42:01, HLA-A*32:15, HLA-A*69:01, HLA-B*08:02, HLA-B*15:09, HLA-A*02:17, HLA-B*08:03, HLA-B*83:01
HCPS_GP2	YAYPWQTAK	94	1.1519	A3	0.4823	0.14992	100.00% (2/2)	100.00% (1/1)	–	–	Non-Toxin	Non-Allergen	3	4	HLA-A*03:01, HLA-A*11:01, HLA-C*03:03, HLA-A*66:01, HLA-C*14:02, HLA-B*14:02
HCPS_GP	RTLGVFTRYK	620	1.5999	A3	1.0703	0.22242	100.00% (7/7)	33.33% (1/3)	100.00% (1/1)	–	Non-Toxin	Non-Allergen	2	5	HLA-A*11:01, HLA-A*03:01, HLA-A*31:01, HLA-A*68:23, HLA-B*15:42, HLA-C*15:02
HCPS_NP	LRYGNVLDV	96	1.2427	B27	1.4139	0.06906	100.00% (39/39)	22.73% (10/44)	72.22% (26/36)	36.96% (17/46)	Non-Toxin	Non-Allergen	2	1	HLA-C*06:02, HLA-B*27:05, HLA-C*07:01
HCPS_RDRPP	L PTRVRLEI	900	1.3724	B7	0.9167	0.20274	100.00% (15/15)	100.00% (9/9)	100.00% (4/4)	100.00% (5/5)	Non-Toxin	Non-Allergen	3	3	HLA-B*51:01, HLA-B*53:01, HLA-B*42:01, HLA-B*83:01, HLA-B*08:02
HFRS_GP1	QCIYTITSL	433	0.6363	A26	0.5673	0.13866	99.40% (165/166)	100.00% (6/6)	–	–	Non-Toxin	Non-Allergen	1	2	HLA-B*39:01, HLA-B*14:02, HLA-B*15:09
HFRS_GP2	KYEYPWHTA	93	0.5453	A24	0.6315	0.27647	99.40% (166/167)	100.00% (6/6)	–	–	Non-Toxin	Non-Allergen	1	2	HLA-A*24:02, HLA-A*32:07, HLA-A*02:50
HFRS_GP	CYGAESVTL	1013	1.2413	A24	0.9011	0.04966	96.45% (190/197)	6.94% (5/72)	94.29% (33/35)	0.00% (0/10)	Non-Toxin	Non-Allergen	1	5	HLA-A*24:02, HLA-A*24:03, HLA-A*23:01, HLA-B*35:03, HLA-C*07:02, HLA-C*04:01
HFRS_NonP	REQWKWTQM	16	1.0668	B44	1.0756	0.14888	66.67% (2/3)	–	–	–	Non-Toxin	Non-Allergen	1	1	HLA-B*40:02, HLA-B*40:01
HFRS_NP	AELGAFFSI	330	1.878	B44	0.6213	0.18094	88.87% (631/710)	28.02% (65/232)	98.00% (49/50)	28.89% (26/90)	Non-Toxin	Non-Allergen	5	2	HLA-B*40:02, HLA-B*44:02, HLA-B*18:01, HLA-A*02:06, HLA-B*40:01, HLA-B*45:01
HFRS_RDRPP	TNAEFLSTF	1167	0.8146	B62	0.4938	0.10007	100.00% (132/132)	100.00% (60/60)	100.00% (5/5)	92.31% (12/13)	Non-Toxin	Non-Allergen	2	2	HLA-B*18:01, HLA-A*24:02, HLA-A*26:02, HLA-A*25:01

**Table 2**Potential CD4<sup>+</sup> T-cell vaccine candidates and their characteristics corresponding to each protein of orthohantavirus.

Protein name	Peptide sequence	Start	Antigenicity score	Conservancy for classified-causative group	Conservancy for classified-unknown group	Conservancy for unclassified-causative group	Conservancy for unclassified-unknown group	Toxicity prediction	IL10 prediction	Allergenicity prediction	Allele	
HCPS_GP1	EGLCFIPTHTIALTQ	168	0.8556	100.00% (2/2)	0.00% (0/1)	–	–	Non-Toxin	IL10 inducer	Non-Allergen	HLA-DRB1*07:01	
HCPS_GP2	ILILSILLFSFFCPI	466	0.5902	100.00% (2/2)	0.00% (0/1)	–	–	Non-Toxin	IL10 inducer	Non-Allergen	HLA-DPA1*02:01/DPB1*05:01, HLA-DPA1*01/DPB1*04:01, HLA-DRB4*01:01, HLA-DQA1*01:01/DQB1*05:01, HLA-DPA1*01:03/DPB1*02:01	
HCPS_GP	VGLVWGILLTTELII	633	0.6975	85.71% (6/7)	0.00% (0/3)	100.00% (1/1)	–	Non-Toxin	IL10 inducer	Non-Allergen	HLA-DPA1*03:01/DPB1*04:02, HLA-DPA1*01:03/DPB1*02:01, HLA-DRB1*09:01, HLA-DPA1*01/DPB1*04:01	
✓	HCPS_NP	PIILKALYMLSTRGR	132	0.9266	89.74% (35/39)	86.36% (38/44)	50.00% (18/36)	67.39% (31/46)	Non-Toxin	IL10 inducer	Non-Allergen	HLA-DRB4*01:01
	HCPS_RDRPP	ADRGFFITTLPTRVR	891	0.6445	100.00% (15/15)	100.00% (9/9)	100.00% (4/4)	80.00% (4/5)	Non-Toxin	IL10 inducer	Non-Allergen	HLA-DRB1*09:01, HLA-DPA1*01/DPB1*04:01, HLA-DRB1*01:01, HLA-DRB1*07:01, HLA-DPA1*03:01/DPB1*04:02
	HFRS_GP1	ALLVTFCFGWVLIPA	468	0.8778	91.57% (152/166)	50.00% (3/6)	–	–	Non-Toxin	IL10 inducer	Non-Allergen	HLA-DQA1*01:01/DQB1*05:01
	HFRS_GP2	VHALGHWFDFGRLNLK	68	0.415	97.01% (162/167)	66.67% (4/6)	–	–	Non-Toxin	IL10 inducer	Non-Allergen	HLA-DQA1*01:01/DQB1*05:01
	HFRS_GP	GCYRTLNLFRYKSRC	611	0.9354	93.91% (185/197)	18.06% (13/72)	100.00% (35/35)	0.00% (0/10)	Non-Toxin	IL10 inducer	Non-Allergen	HLA-DPA1*02:01/DPB1*05:01
	HFRS_NonP	QREQWKWTQMELIKT	15	0.7028	66.67% (2/3)	–	–	–	Non-Toxin	IL10 inducer	Non-Allergen	HLA-DRB1*07:01, HLA-DPA1*02:01/DPB1*01:01
	HFRS_NP	QSYLRRTQSMGIQLD	367	0.5736	97.61% (693/710)	18.53% (43/232)	100.00% (50/50)	27.78% (25/90)	Non-Toxin	IL10 inducer	Non-Allergen	HLA-DRB1*09:01, HLA-DRB1*07:01
	HFRS_RDRPP	TEADRGGFFITTLPTR	888	0.5602	96.97% (128/132)	71.67% (43/60)	100.00% (5/5)	61.54% (8/13)	Non-Toxin	IL10 inducer	Non-Allergen	HLA-DPA1*03:01/DPB1*04:02

**Table 3**  
Potential B-cell vaccine candidates and their characteristics corresponding to each protein of orthohantavirus.

Protein name	Peptide sequence	Start	SVM score	Percent probability of correct prediction	Antigenicity score	Conservancy for classified-causative group	Conservancy for classified-unknown group	Conservancy for unclassified-causative group	Conservancy for unclassified-unknown group	Toxicity prediction	Allergenicity prediction
HCPS_GP1	TPVPIQGQVTDLKIESCNFD	30	0.70815019	73.61	1.3796	100.00% (2/2)	0.00% (0/1)	—	—	Non-Toxin	Non-Allergen
HCPS_GP2	IYSLKYTRKVCIQLGEQTC	148	0.81914362	77.3	1.4872	100.00% (2/2)	0.00% (0/1)	100.00% (1/1)	—	Non-Toxin	Non-Allergen
HCPS_GP	LNRDVSFQDLSDNPKVQDHL	959	0.90270442	80.09	0.6206	100.00% (7/7)	33.33% (1/3)	36.11% (13/36)	41.30% (19/46)	Non-Toxin	Non-Allergen
HCPS_NP	FPAQQRKARNLISPVGMVIGF	206	0.73092054	74.36	0.9974	84.62% (33/39)	86.36% (38/44)	100.00% (9/9)	80.00% (4/5)	Non-Toxin	Non-Allergen
HCPS_RDRPP	YQRTEDRGFFITLPTVRV	886	0.60504896	70.17	0.4233	100.00% (15/15)	100.00% (157/166)	100.00% (6/6)	—	Non-Toxin	Non-Allergen
HFRS_GP1	KQNRFRLTEQQVNFYCQRVD	391	0.6006102	70.02	1.0686	94.58% (157/166)	100.00% (6/6)	—	—	Non-Toxin	Non-Allergen
HFRS_GP2	RIEWKDQDGMLRDHNLVLT	290	0.3364916	61.22	0.7663	97.01% (162/167)	100.00% (6/6)	—	—	Non-Toxin	Non-Allergen
HFRS_GP	KHRMVEEYSYNRNSVCYDL	110	0.3484335	61.62	0.942	27.41% (54/197)	1.39% (1/72)	94.29% (33/35)	0.00% (0/10)	Non-Toxin	Non-Allergen
HFRS_NonP	TRLGNLMLTTSRRDQALGME	67	0.73619828	74.54	1.4148	66.67% (2/3)	—	—	—	Non-Toxin	Non-Allergen
HFRS_NP	SKTVGTAAEKLKRKSFSYQS	349	0.33873278	61.29	0.6994	32.39% (230/710)	13.79% (32/232)	0.00% (0/50)	81.11% (73/90)	Non-Toxin	Non-Allergen
HFRS_RDRPP	ILGSMSDLPGLGYFDLAA	1188	0.50581281	66.86	0.4247	97.73% (129/132)	26.67% (16/60)	80.00% (4/5)	23.08% (3/13)	Non-Toxin	Non-Allergen

in a single FASTA file; where 68 organisms with 2162 proteins were classified and the remaining 44 organisms with 325 proteins were unclassified. The data overview is illustrated in Fig. 1 after rearranging the retrieved sequences according to their category, organism, and epidemic nature. In Fig. 1(a), only 27 organisms (classified: 17, unclassified: 10) with 137 proteins (classified: 88, unclassified: 49) are causative for human HCPS and 23 organisms (classified: 8, unclassified: 15) with 120 proteins (classified: 65, unclassified: 55) are unknown for human infection but associated with HCPS. As opposed to, only 14 organisms (classified: 9, unclassified: 5) with 1700 proteins (classified: 1599, unclassified: 101) are causative for human HFRS and 48 organisms (classified: 34, unclassified: 14) with 530 proteins (classified: 410, unclassified: 120) are unknown for human infection but associated with HFRS. Among 18 protein categories, only the envelope glycoprotein, envelope glycoprotein G1, envelope glycoprotein G2, nucleocapsid protein, RdRp protein, and nonstructural protein from every group were the central target of this study (Fig. S1(a)). The mentioned proteins of the classified causative groups were tested for antigenicity and the 11 highest antigenic proteins were selected as an initial input dataset for epitope prediction and all groups of proteins were used to evaluate the conservancy of the predicted epitopes in order to confirm their cross-protective ability. The summary of the selected highest antigenic proteins are shown in Fig. 1(b) & Fig. S1(b).

### 3.2. Prediction of T-cell epitopes and major histocompatibility complex alleles

The highest antigenic proteins were submitted as input to the NetCTL v1.2 server and in total of 3769 9-mer CTL epitopes with a combined score  $\geq 0.5$  were predicted (Tab. S1). The predicted epitopes were considered to investigate their antigenicity, immunogenicity, conservancy, toxicity, and their respective MHC HLA alleles. Thereafter, the predicted epitopes were filtered according to the antigenicity  $\geq 0.4$ , immunogenicity  $> 0$ , toxicity  $< 0$ , and allele available in PDB  $> 0$  and found that 654 epitopes successfully satisfied all the criteria. Later, these 654 epitopes were tested for their allergenicity and found that only 380 epitopes showed a non-allergic nature. Finally, among those 380 epitopes, the best one epitope from each protein was selected as a vaccine candidate that has characteristics better than others of that protein (Table 1). Again, the highest antigenic proteins were submitted as input to the IEDB MHC II binding tool and in total of 2197 15-mer HTL epitopes were predicted with consensus percentile rank  $\geq 2$  (Tab. S2). The predicted epitopes were tested for their antigenicity, conservancy, and toxicity and found that 1245 epitopes were satisfied antigenicity  $\geq 0.4$  and non-toxin criteria. Afterword, these 1245 epitopes were evaluated for their allergenicity and observed that 771 epitopes were found to be non-allergic. Later, these 771 epitopes were investigated for their IL-10 inducing criteria. The IL-10 is significantly decreased from early to late phase of disease occurred by hantavirus [112]. Finally, the best one epitope from each protein was selected as vaccine candidate that satisfied IL-10 inducing criteria and have other characteristics better than the remaining epitopes of that protein (Table 2). The conservancy of the selected vaccine candidates confirmed their high cross-protective ability.

### 3.3. Prediction of linear B-Lymphocyte vaccine candidates

The selected highest antigenic 11 proteins were submitted to the LBtope server and a total of 2939 20-mer B-lymphocyte epitopes with the percent of probability is 60% were predicted (Tab. S3) and considered for the evaluation of their antigenicity, conservancy, and toxicity. According to the antigenicity  $\geq 0.4$  and non-toxin criteria, only 1789 epitopes have remained and were taken into account for investigating their allergenicity and found that 1011 epitopes have non-allergic nature. Subsequently, among the non-allergic epitopes of each protein, the best one epitope was selected as a vaccine candidate that significantly

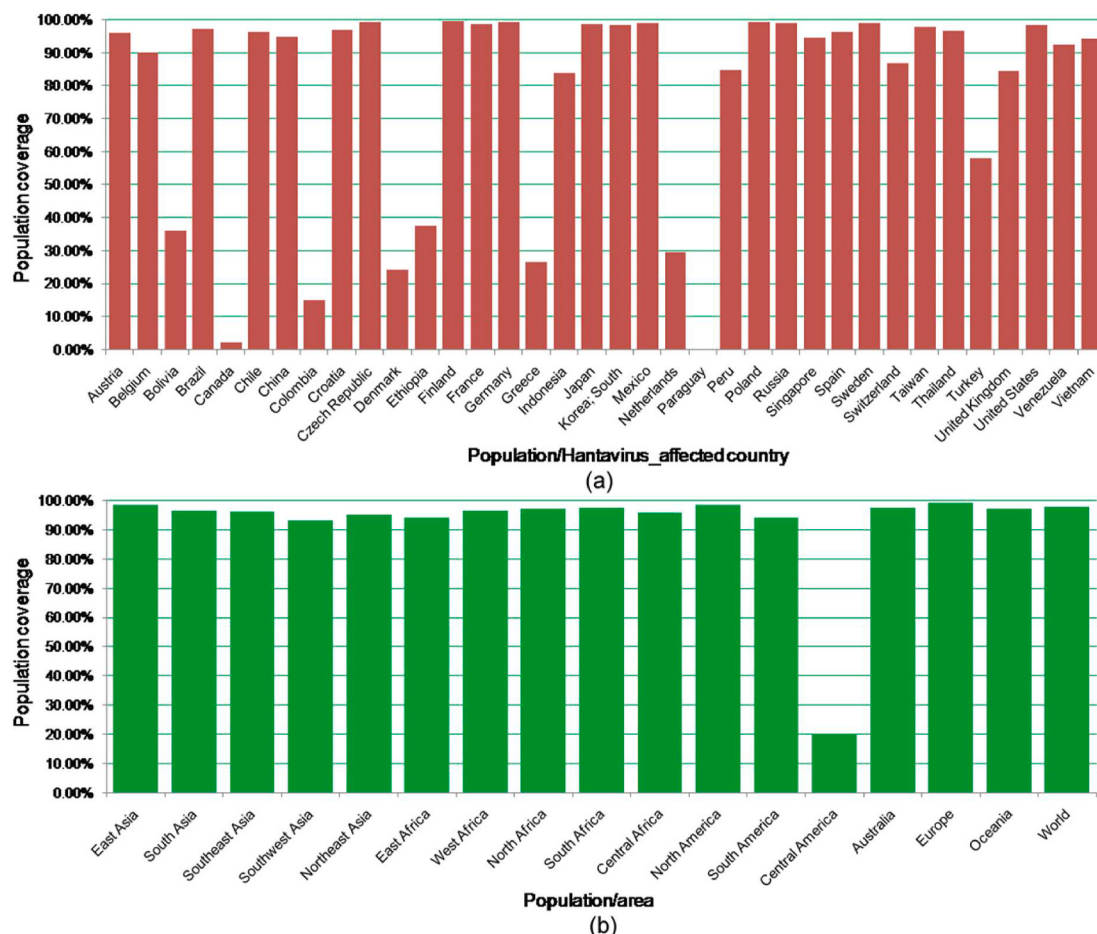


**Fig. 2.** Percentage of population coverage. (a) Percentage of population coverage in the Hantavirus affected countries. (b) Percentage of population coverage in 16 different areas covering the world as well as in the whole world.

satisfies all the characteristics than other epitopes of that protein (Table 3). The high cross-protective ability of the selected vaccine candidates was confirmed by their conservancy results.

#### 3.4. Population distribution analysis

The analysis of population distribution was conducted for the combined of robust CTL & HTL vaccine candidates and their associated HLA alleles. The analysis result showed excellent population coverage in different epidemic and non-epidemic countries, areas, and ethnic groups (Tab. S4). Among epidemic regions, the result revealed the highest coverage of the population in Finland (99.62%), intimately succeeded by Germany (99.45%), Poland (99.31%), Czech Republic (99.27%), Mexico (99.19%), Sweden (99.14%), Russia (98.98%), Japan (98.91%), France (98.86%), England (98.84%), South Korea (98.50%), United States (98.45%), Brazil (97.19%), Thailand (96.63%), and others (Fig. 2(a)). Among 16 broad geographical regions, the maximum cumulative coverage of population in Europe (99.10%), nearly followed by East Asia (98.72%), North America (98.43%), and others (Fig. 2(b)). However, 97.94% of the world's population covered by predicted vaccine candidates (Fig. 2(b)). Therefore, it is concluded that the MHC HLA alleles corresponding to the robust T-cell vaccine candidates are well and widely distributed throughout the world, which is a robust property of rational vaccine design [113,114]. In 1976, Hantaan virus (HTNV) with its reservoir, striped field mouse (*Apodemus agrarius*) of Muridae family were addressed by Lee et al. as the first etiological agent of HFRS in South Korea near to the Hantaan River [115] and later in China and Russia [1]. In 1930s, the milder form of HFRS called Nephropathia

Epidemica (NE) was initially identified in Sweden and occurring thousands cases annually all over the Europe [116] and in 1980, Puumala virus (PUUV) was discovered in bank voles (*Myodes glareolus*) as an etiological agent of NE in Finland [117]. The Puumala virus is also an agent of HFRS and recently identified as an agent of HCPS in Germany [118]. The Seoul virus (SEOV) hosted by rates is the second most significant pathogenic agent of HFRS found predominantly in Korea and worldwide [119,120]. Further, the Dobrava-Belgrade virus (DOBV) [121] and Tula virus (TULV) were found as human pathogenic agents of HFRS in Europe [122]. The causative agent of Thailand virus (THAIV) and THAIV-like virus Anjouzorobe virus (ANJOV) were in Thailand and Madagascar, respectively [7,123–125]. Heinemann et al. reported the Bowe virus (BOWV) as HFRS related human pathogenic agent [2] and also the Sangassouvirus (SANGV) have described as HFRS agents and found in West Africa (Guinea) [126]. In contrast, the Sin Nombre virus (SNV) and Andes virus (ANDV) were discovered as etiological agents of HCPS in North and South America, respectively [1,127] where only ANDV has the characteristics of person-to-person transmission. Subsequently, there are about 43 strains have been identified in the Americas and 20 strains of them can develop human disease [1]. In Brazil, the Araraquara virus (ARAV) is a top virulent agent of HCPS with 50% fatality rate [21]. Furthermore, HCPS was also reported as the consequence of Bayou virus (BAYV), Lechiguanas virus (LECV), Black Creek Canal virus (BCCV), Hu39694 virus, Choclo virus (CHOV), Bermejo virus (BMJV), Oran virus (ORNV), Laguna Negra virus (LNV), Neembucu virus, Cano Delgadito virus (CADV), Tunari virus, Maciel virus (MCLV), Blue River virus, and El Moro Canyon virus (ELMCV) [1,23, 128–130].

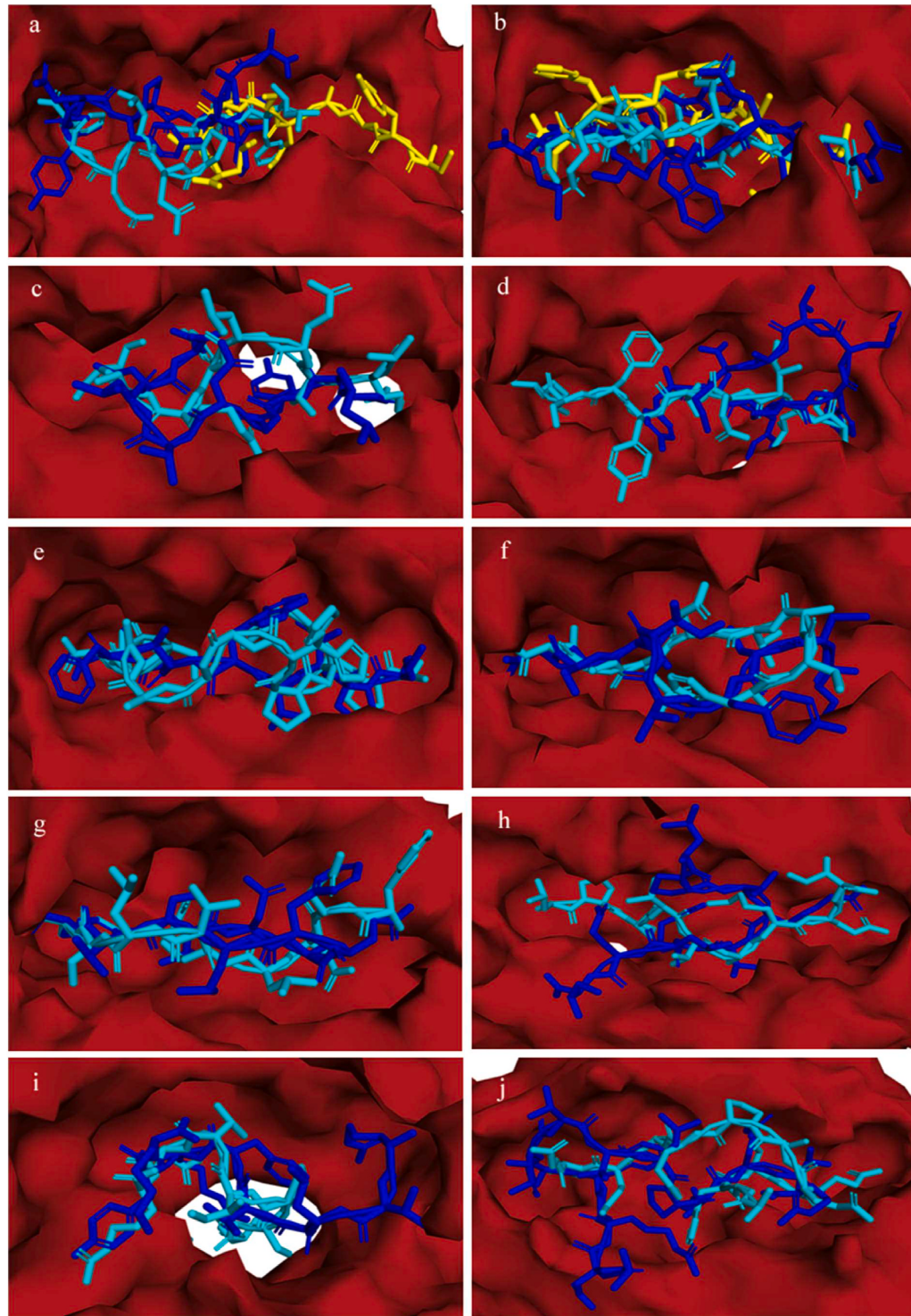


**Fig. 3.** Epitope-allele docked complexes. In all the figures, firebrick color represents the allele protein, cyan color indicates the experimental ligand, and blue & yellow colors highlight the epitopes. The figure (a) shows the docked complexes of HLA-A2402 with HFRS\_GP2-CTL\_Epitope (blue) and HFRS\_GP-CTL\_Epitope (yellow) and the figure (b) shows the docked complexes of HLA-B4002 with HFRS\_GP-CTL\_Epitope (blue) and HFRS\_NP-CTL\_Epitope (yellow). The figures (c–i) highlight the docked complexes of HLA-C0602, HLA-A0301, HLA-B0702, HLA-B3901, HLA-B1801, HLA-B5101, and HLA-A1101 with HCPS\_NP-CTL\_Epitope, HCPS\_GP2-CTL\_Epitope, HCPS\_GP1-CTL\_Epitope, HFRS\_GP1-CTL\_Epitope, HCPS\_NonP-CTL\_Epitope, and HCPS\_GP-CTL\_Epitope, respectively. The figure (j) shows the docked complex between HLA\_DRB1\_0101 and HFRS\_NP-CTL\_Epitope.

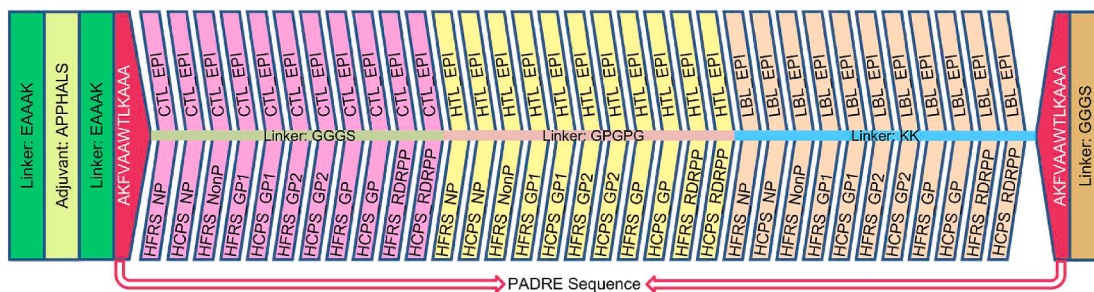


**Fig. 4.** Schematic diagram of the multi-epitope subunit vaccine construct. An adjuvant (TLR-4 agonist: APPHALS) was added at the N-terminal site of the construct with the help of EAAAK linker and the CTL, HTL, and LBL epitopes were merged with the help of GGGGS, GPGPG, and KK linkers, respectively.

### 3.5. Molecular docking analysis of MHC HLA alleles-peptides interactions

The binding ability of the predicted vaccine candidates with their associated MHC HLA alleles should be checked for their robustness. The molecular dockings of the peptide-allele complexes were done through AutoDock & AutoDockVina and the docking scores were compared with their control scores (Fig. S2). The vaccine candidates exhibited excellent binding energy with their respective HLA-alleles. Specifically, the binding score of the epitope YAYPWQTAK is equal to its control score of  $-7.6$ . In addition, the epitopes QCIYTITSL, LRYGNVLDV, REQWKWTQM, and ADRGFFITTLPTRVR have binding scores of  $-7.9$ ,  $-7.5$ ,  $-8.5$ ,  $-6.8$ , that are close proximity of their respective control scores of  $-8.0$ ,  $-7.3$ ,  $-8.6$ ,  $-6.6$ , respectively. The epitope-allele docked complex structures were shown in Fig. 3.

### 3.6. Clustering of the MHC-Restricted HLA alleles

The MHCcluster v2.0 server can generate a correlation heat-map for clustering both the MHC-I and MHC-II HLA molecules interacted with the robust vaccine candidates. The generated heat-map is illustrated in Fig. S3 showing a satisfactory functional relationship among detected allele molecules as the red-colored zones indicating strong correlation and gradually yellow-colored zones indicating weaker correlation [75].

### 3.7. Multi-epitope subunit vaccine protein construction

The immune response plays a critical role in fighting viral infections and its molecular and cellular mechanisms induced by the multi-epitope vaccine [24]. Therefore, extracted robust vaccine candidates of total 11 CTL, 11 HTL, and 11 LBL epitopes were sequentially fused together with the help of suitable linkers to construct the long chain of multi-epitope vaccine protein. The linkers GGGGS, GPGPG, and KK were utilized to connect the intra-CTL, intra-HTL, and intra-BL epitopes, respectively. As the length of multi-epitope vaccine is longer than traditional vaccine, it must contain a powerful immunostimulatory adjuvant for enhancing the immunogenicity and activating long-lasting innate and adaptive immune response [24,80]. Finally, four vaccine models of length 654, 692, 686, and 777 amino acids were designed by adding TLR-4 agonist,  $\beta$ 3-defensin,  $\beta$ 3-defensin with RR residues, and 50S ribosomal protein L7/L12 as adjuvants using EAAAK linker, respectively. The lengths of designed vaccine models are not too long comparing to the other developed multi-epitope vaccine against *Fasciola gigantica*, *Schistosoma mansoni*, and *Onchocerca volvulus* of length 765, 617 and 599, respectively [111,131,132]. Shanmugam et al. reported that synthetic TLR-4 can be used as a novel adjuvant [133]. The  $\beta$ -defensin can recruit the Naïve T-cell ( $T_h0$  cell) & immature dendritic-cells (DC) at infection site by the C-C chemokine receptor type 6 (CCR6) receptor and it can also provide innate & adaptive immune response in microbial infection [134]. The 50S ribosomal protein L7/L12 act as an immunoadjuvant for dendritic-cell based immunotherapy and it is capable of inducing dendritic-cell maturation [135]. The sequential vaccine diagram is

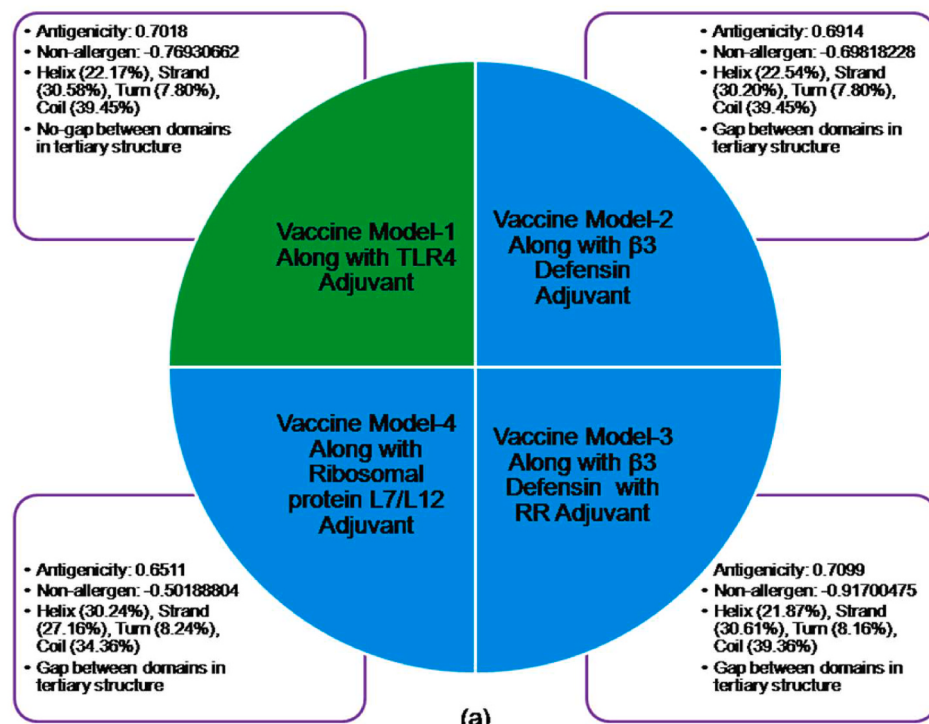
presented in Fig. 4. A major problem of vaccine proteins is the crossing of cellular membranes [136]. However, the Cell-penetrating peptides (CPPs) are short peptides (fewer than 30 residues) and that are able to cross biological membranes without clear toxicity and facilitate the intracellular delivery of a variety of substances into cellular compartments and also capable of enhancing the immunogenic properties [137]. The viral particles (VPs) are best CPPs as that are safe, easy to manipulate, inherently biocompatible, biodegradable, and capable of transporting various substances into specific cells [138]. Therefore, to overcome the problem of crossing cellular membrane, it is suggested to add a linker called the first CPP TAT protein derived from transactivating regulatory protein of Human Immunodeficiency Virus (HIV) [139].

### 3.8. Immunological comparison of the designed vaccine models

Immunological properties such as antigenicity and allergenicity were evaluated for all vaccine models, and the results were illustrated in Fig. 5 (a). The high antigenicity indicates the better ability to provoke immune response. The non-allergic vaccine is completely safe for human life because vaccine with allergic behavior creates various health difficulties [51]. All the vaccine models showed antigenic and non-allergic in nature. Although the vaccine model-3 was characterized by higher antigenicity of 0.7099 & non-allergen score of  $-0.917$ , the vaccine model-1 showed antigenicity of 0.7018 which is very close to the antigenicity of vaccine model-3. Ali et al. designed a vaccine model against dengue whose antigenicity score was 0.6251 predicted by VaxiJen server and also the vaccine model had shown the non-allergen property [26].

### 3.9. Structural comparison of the designed vaccine models

The characteristics of the constructed vaccine secondary structures were evaluated by SOPMA server utilizing their peptide sequences. The predicted results were illustrated in Fig. 5(a). Thereafter, the vaccine models were submitted to RaptorX server for predicting their 3D structures. The predicted results were checked for the gap between domains of the predicted 3D models and observed that only the vaccine model-1 exhibited no gap between domains (Fig. 5(a)). The 3D protein models having a gap between domains create problems in the refining stage of those models [86]. Therefore, the vaccine model-1 was selected as the final vaccine construct for further immunoinformatics approaches. From the SOPMA output, the probability scores of occurrence of every secondary structure at each residue of the designed final vaccine sequence were shown in Fig. S4, where the structure associated with highest score at each position is finally predicted secondary structure at that position. The 3D model of the constructed final vaccine protein was predicted as 2 domains (5j81:A, 4ind:A) and modelled using 4ind:A as the best template with a score of 50. All of the 654 amino acids were modelled, but 10% of residues were predicted as disordered. The p-value and uGDT value are the quality measures in homology modelling, lower p-value and higher uGDT value confirm the quality of the



(a)



(b)

**Fig. 5.** Immunological and tertiary structural properties of the vaccine constructs. (a) Comparison of the vaccine models by immunological and structural properties. (b) Physicochemical properties of the finally selected vaccine model-1.

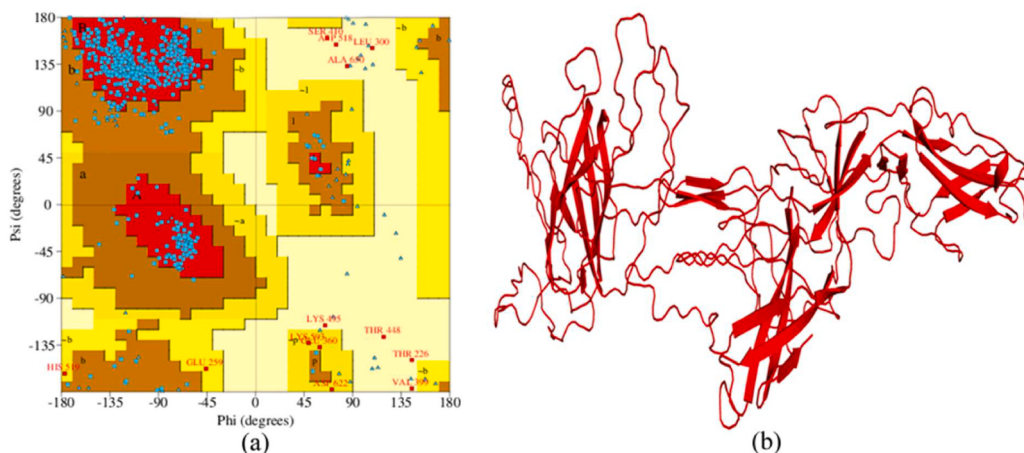


**Fig. 6.** Structural assessment of the final vaccine construct. (a) Ramachandran plot of the refined model showing 86.2%, 11.3%, 1.0%, and 1.3% residues were found in most Rama-favored regions, additional allowed regions, generously allowed regions, and disallowed regions respectively. (b) Refined 3D structure of the final vaccine construct.

modelled structure [84]. The *p*-value and uGDT values obtained for the modelled structure were  $8.84 \times 10^{-5}$  and 120, respectively, which are sufficiently low and large, respectively. Many researchers reported the tertiary structure quality parameter *p*-value for their designed multi-epitope vaccine model against dengue and HIV were  $1.80 \times 10^{-3}$  and  $4.18 \times 10^{-3}$ , respectively [26,79].

### **3.10. Refinement and quality assessment of the tertiary structure of the final vaccine construct**

Structural refinement with GalaxyRefine can improve structural quality by increasing the number of amino acids in the favored region. GalaxyRefine generated five refined models. The quality parameters of the refined models are shown in Tab. S5. Comparing the quality parameters, the refined model 4 was considered as the best refined tertiary structure of the designed final vaccine protein. The refined model 4 showed GDT-HA (0.9209), RMSD (0.502), MolProbity (2.432), Clash score (28.6), Poor rotamers (0.8), and Rama favored (91.9). The Ramachandran plot analysis was carried out to validate the structure of refined model 4 and found that 86.2%, 11.3%, 1.0%, and 1.3% amino acids in Rama-favored regions, additionally allowed regions, generously allowed regions, and disallowed regions, respectively (Fig. 6(a)). The ERRAT server helps to compute the overall quality factor of the selected refined model and it was 52.13%. Later on, the ProSA-web was runned with the selected refined model and the determined Z-score of -3.51 is

The refined 3D model is illustrated in Fig. 6(b).

### *3.11. Assessment of primary sequence features of the final vaccine construct*

Several primary sequence features of the designed final vaccine protein were determined by ExPASy ProtParam server (Fig. 5(b)). The molecular weight was 70.5 kDa which characterize the vaccine construct as good antigenic vaccine candidate [78]. The good vaccine candidates should have the molecular weight <110 kD [140]. The vaccine buffer system is crucial at purification stage and isoelectric point (pI) is the measure of pH value for buffer system. The pI value of 10 predicted the vaccine construct as slightly basic in nature. Moreover, the estimated half-life results showed 1 h in mammalian reticulocytes (*in vitro*); while 30 min & >10 h in yeast & *E. coli* (*in vivo*), respectively. The instability index was assessed to be 32.04, which categorize the vaccine construct as stable [91]. The aliphatic index was determined to be 76.22 which classify the vaccine construct as thermostable; the higher aliphatic index is the indication of greater thermostability [80]. The estimated GRAVY value of -0.255 indicated that the vaccine construct has excellent interaction with a water molecule [80]. The SOLpro tool was also showed that the vaccine construct is soluble with probability 0.93. Pandey *et al.* reported their designed HIV vaccine model with molecular weight, theoretical pI, aliphatic index, and GRAVY value of

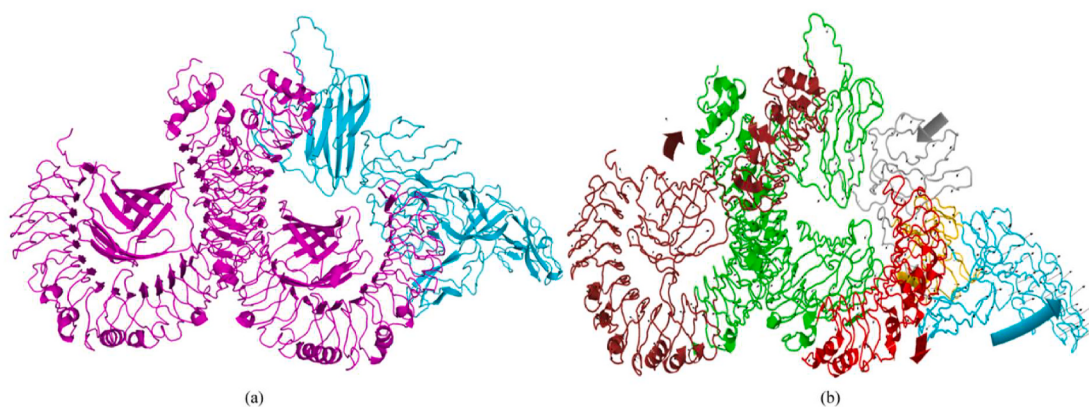


**Fig. 7.** The vaccine-receptor complexes. (a) The docked complex of the vaccine construct with the TLR-4 receptor (cyan color represent the vaccine construct and magenta color represent the TLR-4 receptor). (b) The docked complex after dynamics simulation. The large arrows indicate the direction of the vaccine protein and receptor TLR-4 towards each other. The small arrows indicate the direction of the residues where the length of the line indicates the degree of mobility.

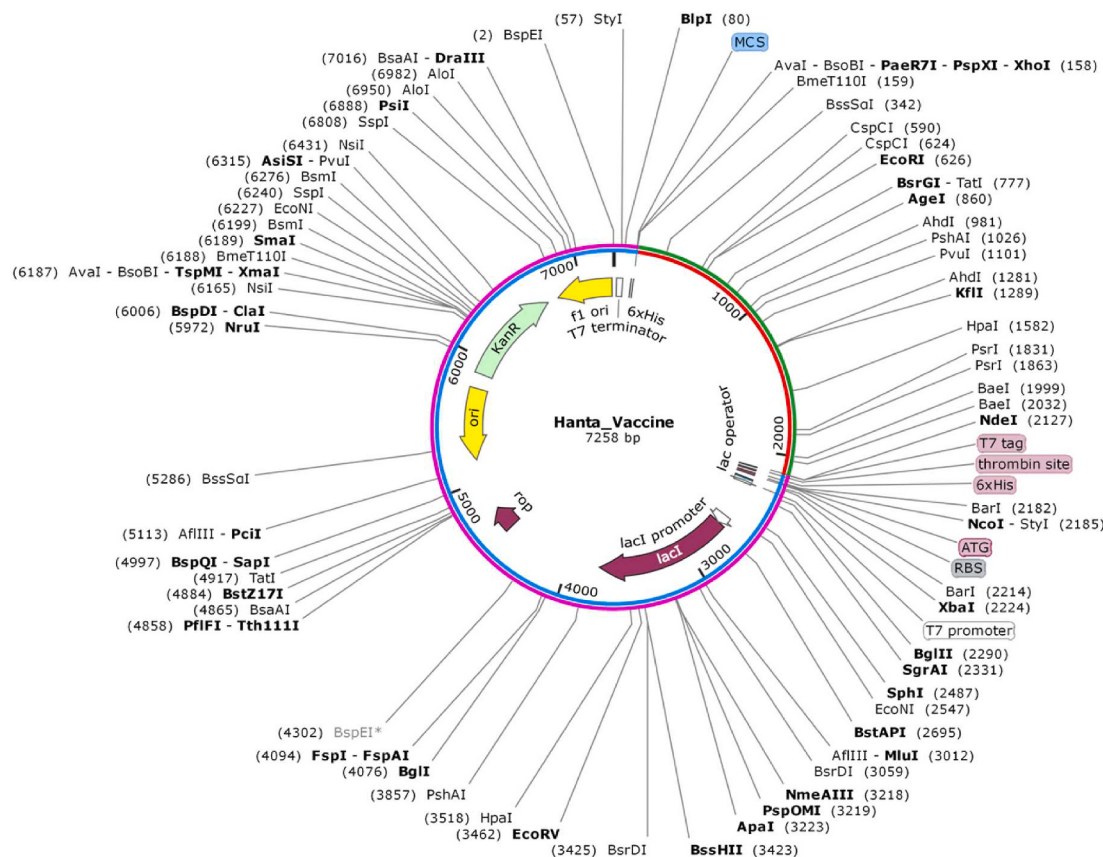


**Fig. 8.** Cloned multi-epitope vaccine construct. *In silico* cloning of the adapted codon sequence of the final vaccine construct (red-green color) into the *E. coli* pET28a (+) vector (blue-magenta color).

70.8 kDa, 10.01, 94.93, and –0.277, respectively [79].

### 3.12. Mapping of discontinuous B-cell epitopes in designed final vaccine protein

In designing peptide vaccine, conformational B-cell epitopes play vital role in antibody production and the B-cells are central part of humoral immunity [80]. The discontinuous B-cell epitopes were searched in the constructed final vaccine protein using the IEDB ElliPro tool and found 10 significant discontinuous B-cell epitopes with length range 4–110 and score range 0.557–0.811 (Tab. S6). The structural view of those epitopes was illustrated in Fig. S6.

### 3.13. Disulfide engineering of the final vaccine construct

To stabilize the designed vaccine structure, Disulfide by Design 2 (DbD2) runned with the constructed vaccine 3D structure and predicted an aggregate of 70 pairs of amino acids for the likely formation of disulfide bonds (Tab. S7). However, only 5 pairs of residues (Gly344–Ile507, Arg184–Pro265, Thr401–Gly436, Tyr413–Glu556, and Ala270–Pro375) were selected for the disulfide bond formation since their energy and Chi3 values are within the acceptable range i.e. the energy score should be less than 2.2 and the Chi3 value should be between –87 and +97 [94]. Thereafter, the stability of the vaccine structure for the mutation of every residue by cysteine in the selected 5 pairs was evaluated through DynaMut server and found that only three mutations of Gly344, Thr401, & Gly436 residues have positive vibrational entropy changes, which indicates the stability of the vaccine construct (Tab. S8). Among those three residues, Thr401 and Gly436 fulfil a pair for probable disulfide bond. Therefore, these two residues, Thr401 and Gly436 were taken into account for the mutation with cysteine (Fig. S7).

### 3.14. Vaccine-receptor molecular docking

The ClusPro v2.0 server assessed the binding affinity of the designed vaccine protein with TLR-4 receptor by conducting their docking and also provided an aggregate of 26 complex structures (Tab. S9). Among them, the model having the lowest energy score occupied the receptor properly [79] and accordingly the model number 11 was picked out as the best docked complex with lowest energy score of –1292 kJ/mol (Fig. 7(a)). The energy score is inversely related to the binding interaction. The docking task between the vaccine construct and receptor protein was also done through PatchDock software and the results were refined by FireDock. However, the best refined model has the lowest global energy score of –44.68, attractive VdW of –26.77, repulsive VdW of 24.70, ACE of –4.54, and HB of –2.36. In 2018, Pandey et al. reported that the designed multi-epitope vaccine model against HIV had shown the lowest energy score of –1553.7 kJ/mol for ClusPro result and the lowest global energy score of –14.7 for PatchDock result refined by FireDock [79].

### 3.15. Molecular dynamics simulation of the best vaccine-receptor docked complex

The stability and large-scale mobility of the best vaccine-receptor docked complex were investigated by performing normal mode analysis (NMA) of its internal coordinates via iMODS. The vaccine protein and the receptor TLR-4 were directed towards each other and each residue direction was represented by arrows (Fig. 7(b)); where the line-length indicates the degree of mobility. The vaccine-receptor complex deformability depends on the individual distortion of each residue, indicated by hinges in the high deformability region of the chain (Fig. S8 (a)). The B-factor values deduced via NMA was equivalent to root mean

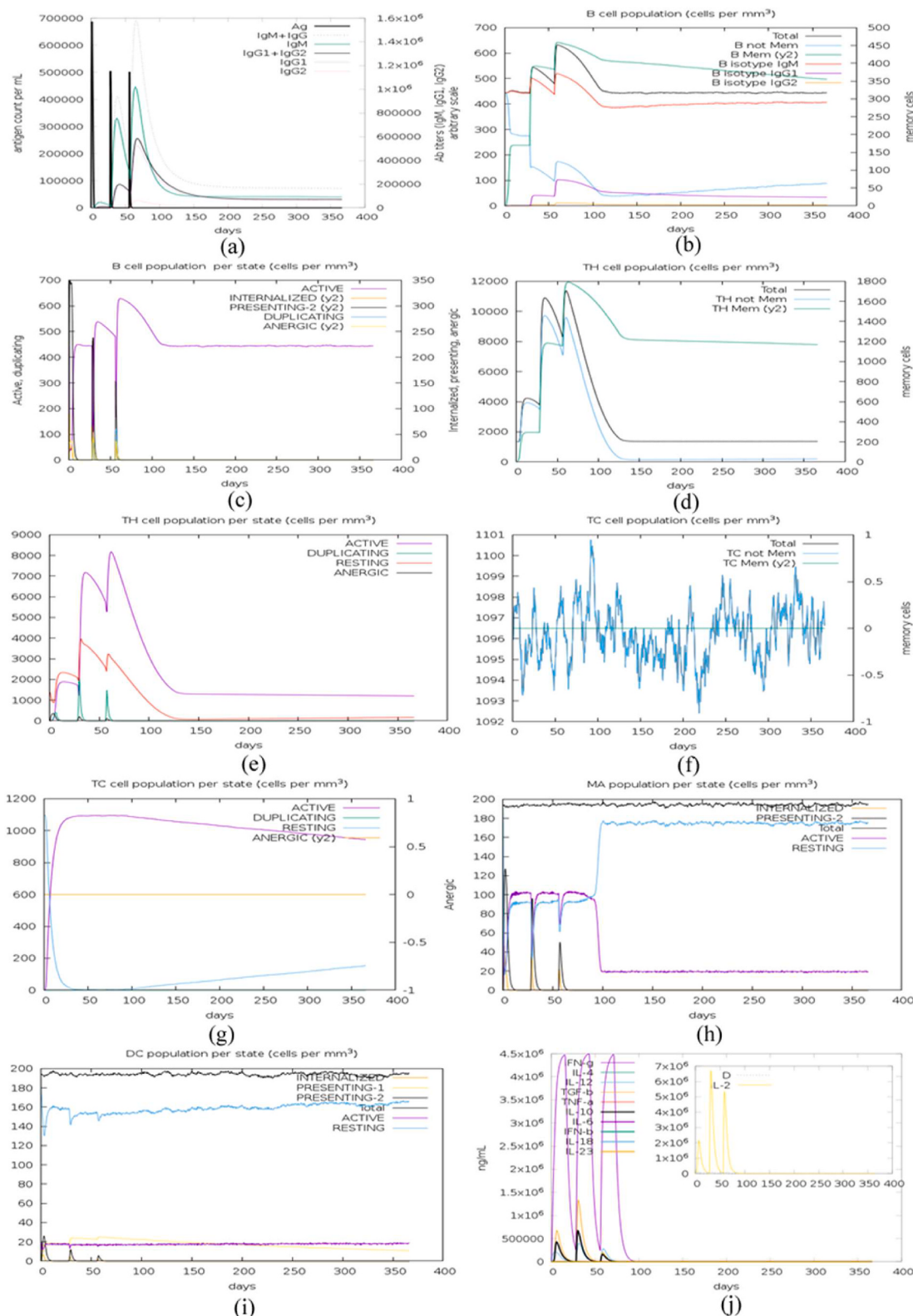


**Fig. 9.** *In silico* simulation of immune response after injecting three injections by 4-weeks apart. (a) Antigen and immunoglobulins (antibodies are sub-divided per isotype). (b) B-lymphocytes count. (c) B-lymphocytes count per entity-state. (d) CD4 T-helper lymphocytes count. (e) CD4 T-helper lymphocytes count per entity-state. (f) CD8 T-cytotoxic lymphocytes count. (g) CD8 T-cytotoxic lymphocytes count per entity-state. (h) Macrophages count per entity-state. (i) Dendritic cell (DC) can present antigenic peptides on both MHC class-I and class-II molecules (the curves show the total number broken down to active, resting, internalized, and presenting the Ag). (j) Concentration of cytokines and interleukins. Simpson index (D) in the inset plot is danger signal.

square (RMS) (Fig. S8(b)). The complex eigenvalue was found to be  $5.608279 \times 10^{-6}$  (Fig. S8(c)); where the lower eigenvalue indicates the easier deformation [107]. The eigenvalue is inversely related to the variance of the complex (Fig. S8(d)) [141]. In the covariance matrix, the red, white, and blue colors indicate the correlated, uncorrelated, and anti-correlated pairs of residues (Fig. S8(e)) [107,142]. An elastic network model was generated to represent the pair of atoms connected via springs (Fig. S8(f)). In the elastic graph, each dot represents one spring between the corresponding pair of atoms, where the darker grays indicate stiffer springs and vice versa [107]. All the results summarises the good stability of the best vaccine-receptor docked complex structure.

### 3.16. In silico cloning of the final vaccine construct

The *in silico* cloning was carried out to confirm the expression rate of the designed vaccine protein into the *E. coli* expression system. To do this, the codon sequence of vaccine protein in accordance with *E. coli* K12 was obtained by JCcat server. This server predicted a optimized DNA sequence of 1962 nucleotides with CAI value of 0.98 and the percentage of the GC-content codon of 53.77%. The calculated CAI value and the percentage of the GC-content codon lies between their respective allowable range 0.8–1.0 and 30–70%, respectively and assured that the designed vaccine protein has high expression rate in *E. coli* K12 [26]. The closer CAI value of 0.986 and the GC content of adapted codons of 51.97% were predicted for the designed multi-epitope vaccine against HIV by Pandey et al. [79]. Subsequently, the expected cloned vaccine of 7258 base pairs was obtained by inserting the optimized DNA sequence into the *E. coli* pET28a(+) vector (Fig. 8).

### 3.17. In silico immune simulation of final vaccine protein

The *in silico* immune response of the vaccine construct was generated by C-ImmSim immune simulator. The immune simulation results exhibited that the designed vaccine construct has the ability to induce a typical immune response (Fig. 9). The primary response of the vaccine construct was confirmed by high levels of immunoglobulin M (IgM). Subsequently, the secondary and tertiary responses were assured by the high level of various antibodies such as immunoglobulin M (IgM), immunoglobulin G (IgG) + immunoglobulin M (IgM), and immunoglobulin G1 (IgG1) + immunoglobulin G2 (IgG2) with decreasing antigen concentration (Fig. 9(a)). The hantavirus infection is confirmed by positive anti-hantavirus IgG/IgM [112]. Furthermore, there are several long-lasting B-cell isotypes and found that possible isotype switching potentials and memory formation (Fig. 9(b and c)). Also the HTL and CTL cell populations indicate the high response with respective memory development (Fig. 9(d-g)). There are increased macrophage and dendritic cell activity were demonstrated as consistent during exposure (Fig. 9(h and i)). These cells are influential for TLR-4 expression in human [143]. In addition, the high levels of IFN- $\gamma$  & IL-2 were also apparent and the smaller Simpson index (D) is associated with greater diversity (Fig. 9(j)) [109]. In addition, there are many other characteristics have been produced such as plasma lymphocyte B (PLB) cell population, regulatory T (TR) cell population per state, natural killer (NK) cell population, and epithelial (EP) cell population per state (Fig. S9); where all of them showed excellent immune response. In addition, repeated exposure with 12 injections evoked an increasing level of IgG1 and IgM, while the high level of IFN- $\gamma$  & TH cell populations were maintained all over the duration of exposure (Fig. S10). The high production of IFN- $\gamma$  and IL-2 cytokines during repeated exposure confirms the efficient Ig production, thereby, supporting a humoral response [111]. This profile indicates the immune memory development and consequently the increased clearance of the antigen at subsequent exposures.

## 4. Conclusion

Infection with zoonotic hantavirus has become a major life-threatening global problem characterized by an increasing number of 50% infections and fatalities worldwide. However, there is currently no permanent cure or preventative treatment for hantavirus. Therefore, it is urgent to develop an effective hantavirus vaccine to combat this serious problem. This study harnessed a complete set of immunoinformatics techniques to develop a cross-protective multi-epitope-based subunit vaccine containing T & B-cell epitopes so that it can induces both of cross-protective cellular and humoral immunity. The T & B-cell epitopes were predicted from the selected highly antigenic proteins of every gene product. The predicted epitopes were filtered by antigenicity  $\geq 0.4$  & immunogenicity  $> 0$  and followed by filtering by the non-toxin & non-allergic criterions. In addition, the helper T-cell epitopes were over-filtered by IL-10 inducing criterion. Furthermore, the top conservancy associated epitope from every gene product was selected as potential vaccine candidate for its better cross-protective ability; among those the T-cell vaccine candidates along with their HLA alleles were subjected to analysis of the population coverage in both the epidemic and non-epidemic regions. Thereafter, the potential vaccine candidates were linked together with the help of suitable linkers for their adequate separate functions in the human body. Subsequently, four vaccine models were generated by adding four different adjuvants to the nascent vaccine protein to increase the vaccine immunogenicity. The vaccine models were tested and compared for its antigenicity and allergenicity and followed by the structural analysis. Further, the physicochemical behaviors of the final vaccine protein were assessed and followed by the discontinuous B-cell epitope prediction. Furthermore, disulfide engineering was executed to intensify the vaccine stability. Molecular docking and dynamics simulation were also carried out to investigate the binding affinity with immune receptor TLR-4 and stability of the vaccine-receptor complex, respectively and followed by conducting *in silico* cloning to confirm the constructed vaccine expression rate. At last, the immune simulation was done to ensure the immune response and antigen clearance rate. However, this recommended vaccine construct requires experimental validation for ensuring the cross-protective immunity against hantavirus.

## Author contributions

FA and UKA planned & designed the protocol; FA and UKA prepared the data; FA performed the computational analysis; FA and ZN prepared the results; FA, SBS and MSAK contributed to screen the vaccine candidates; FA and UKA wrote the manuscript; MMH critically revised the manuscript; UKA supervised the whole study.

## Funding

For this research, the researchers received no specific grant from any funding agencies in the public, commercial, or not-for-profit sectors.

## Declaration of competing interest

The researchers strictly declare that there is no potential conflict of interests regarding the publication of this research article.

## Acknowledgements

All persons who have made substantial contributions to the work reported in the manuscript (e.g., technical help, writing and editing assistance, general support), but who do not meet the criteria for authorship, are named in the Acknowledgements and have given us their written permission to be named. If we have not included an Acknowledgements, then that indicates that we have not received substantial contributions from non-authors.

## Appendix A. Supplementary data

Supplementary data to this article can be found online at <https://doi.org/10.1016/j.micpath.2020.104705>.

## References

- [1] H. Jiang, X. Zheng, L. Wang, H. Du, P. Wang, X. Bai, Hantavirus infection: a global zoonotic challenge, *Virol. Sin.* 32 (2017) 32–43, <https://doi.org/10.1007/s12250-016-3899-x>.
- [2] P. Heinemann, M. Tia, A. Alabi, J.-C. Anon, B. Auste, S. Essbauer, A. Goniñasahé, H. Kignimlman, B. Klempa, C. Kraef, N. Kruger, F.H. Leendertz, M. Ndhatz-Sanogo, F. Schaumburg, P.T. Witkowski, C.G. Akoua-Koffi, D.H. Kruger, Human infections by non-rodent-associated hantaviruses in Africa, *J. Infect. Dis.* 214 (2016) 1507–1511, <https://doi.org/10.1093/infdis/jiw401>.
- [3] R.L. Brocato, J.W. Hooper, Progress on the prevention and treatment of hantavirus disease, *Viruses* 11 (2019) 1–14, <https://doi.org/10.3390/v11070610>.
- [4] M.H. D'Souza, T.R. Patel, Biodefense implications of new-world hantaviruses, *Frontiers in Bioengineering and Biotechnology* 8 (2020) 1–20, <https://doi.org/10.3389/fbioe.2020.00925>.
- [5] Y.-Z. Zhang, Discovery of hantaviruses in bats and insectivores and the evolution of the genus Hantavirus, *Virus Res.* 187 (2014) 15–21, <https://doi.org/10.1016/j.virusres.2013.12.035>.
- [6] W.-P. Guo, X.-D. Lin, W. Wang, J.-H. Tian, M.-L. Cong, H.-L. Zhang, M.-R. Wang, R.-H. Zhou, J.-B. Wang, M.-H. Li, J. Xu, E.C. Holmes, Y.-Z. Zhang, Phylogeny and origins of hantaviruses harbored by bats, insectivores, and rodents, *PLoS Pathog.* 9 (2013), e1003159, <https://doi.org/10.1371/journal.ppat.1003159>.
- [7] J.-M. Reynes, N.K. Razafindralambo, V. Lacoste, M.-M. Olive, T.A. Barivel, V. Soarimalala, J.-M. Heraud, A. Lavergne, Anjozorobe hantavirus, a new genetic variant of Thailand virus detected in rodents from Madagascar, *Vector Borne and Zoonotic Diseases, Larchmont, N.Y.* 14 (2014) 212–219, <https://doi.org/10.1089/vbz.2013.1359>.
- [8] W. Jiang, P. Wang, H. Yu, Y. Zhang, K. Zhao, H. Du, X. Bai, Development of a SYBR Green I based one-step real-time PCR assay for the detection of Hantaan virus, *J. Virol Methods* 196 (2014) 145–151, <https://doi.org/10.1016/j.jviromet.2013.11.004>.
- [9] C.B. Jonsson, L.T.M. Figueiredo, O. Vapalahti, A global perspective on hantavirus ecology, epidemiology, and disease, *Clin. Microbiol. Rev.* 23 (2010) 412–441, <https://doi.org/10.1128/CMR.00062-09>.
- [10] R. ul Khalil, Man Dies of Hantavirus in China: Report, Anadolu Agency, 2020. <https://www.aa.com.tr/en/asia-pacific/man-dies-of-hantavirus-in-china-report/1777762#>.
- [11] L.-X. Zou, M.-J. Chen, L. Sun, Haemorrhagic fever with renal syndrome: literature review and distribution analysis in China, *Int. J. Infect. Dis.* 43 (2016) 95–100, <https://doi.org/10.1016/j.ijid.2016.01.003>.
- [12] W.-Y. Zhang, L.-Y. Wang, Y.-X. Liu, W.-W. Yin, W.-B. Hu, R.J.S. Magalhaes, F. Ding, H.-L. Sun, H. Zhou, S.-L. Li, U. Haque, S.-L. Tong, G.E. Glass, P. Bi, A.C. A. Clements, Q.-Y. Liu, C.-Y. Li, Spatiotemporal transmission dynamics of hemorrhagic fever with renal syndrome in China, 2005–2012, *PLoS Neglected Trop. Dis.* 8 (2014) e3344, <https://doi.org/10.1371/journal.pntd.0003344>.
- [13] H. Jiang, H. Du, L.M. Wang, P.Z. Wang, X.F. Bai, Hemorrhagic fever with renal syndrome: pathogenesis and clinical picture, *Frontiers in Cellular and Infection Microbiology* 6 (2016) 1, <https://doi.org/10.3389/fcimb.2016.00001>.
- [14] S. Zhang, S. Wang, W. Yin, M. Liang, J. Li, Q. Zhang, Z. Feng, D. Li, Epidemic characteristics of hemorrhagic fever with renal syndrome in China, 2006–2012, *BMC Infect. Dis.* 14 (2014) 384, <https://doi.org/10.1186/1471-2334-14-384>.
- [15] A. Papa, A. Vaheri, J.W. LeDuc, D.H. Krüger, T. Avšič-Županc, J. Arikawa, J.-W. Song, A. Markotić, J. Clement, M. Liang, D. Li, L.N. Yashina, C.B. Jonsson, C. Schmaljohann, Meeting report: tenth international conference on hantaviruses, *Antivir. Res.* 133 (2016) 234–241, <https://doi.org/10.1016/j.antiviral.2016.08.015>.
- [16] G. Onishchenko, E. Ezhlova, Epidemiologic surveillance and prophylaxis of hemorrhagic fever with renal syndrome in Russian Federation, *Zhurnal Mikrobiologii, Epidemiologii, i Immunobiologii*, 2013, pp. 23–32.
- [17] D.H. Krüger, R.G. Ulrich, J. Hofmann, Hantaviruses as zoonotic pathogens in Germany, *Deutsches Arzteblatt International* 110 (2013) 461–467, <https://doi.org/10.3238/arztebl.2013.0461>.
- [18] R. Demeester, E. Bottieau, M. Van Esbroeck, M.R. Pourkarim, P. Maes, J. Clement, Hantavirus nephropathy as a pseudo-import pathology from Ecuador, *Eur. J. Clin. Microbiol. Infect. Dis.* 29 (2009) 59, <https://doi.org/10.1007/s10096-009-0820-7>.
- [19] B. Knust, P.E. Rollin, Twenty-year summary of surveillance for human hantavirus infections, United States, *Emerg. Infect. Dis.* 19 (2013) 1934–1937, <https://doi.org/10.3201/eid1912.131217>.
- [20] M. Goeijenbier, F. Aron, F. Anfasa, Å. Lundkvist, J. Verner-Carlsson, C.B.E. M. Reusken, B.E.E. Martina, E.C.M. van Gorp, L. Resida, Emerging viruses in the republic of Suriname: retrospective and prospective study into chikungunya circulation and suspicion of human hantavirus infections, 2008–2012 and 2014, *Vector Borne Zoonotic Dis.* 15 (2015) 611–618, <https://doi.org/10.1089/vbz.2015.1798>.
- [21] L.T.M. Figueiredo, W.M. de Souza, M. Ferrés, D.A. Enria, Hantaviruses and cardiopulmonary syndrome in South America, *Virus Res.* 187 (2014) 43–54, <https://doi.org/10.1016/j.virusres.2014.01.015>.
- [22] B. Armien, J.M. Pascale, C. Muñoz, J. Mariñas, H. Núñez, M. Herrera, J. Trujillo, D. Sánchez, Y. Mendoza, B. Hjelle, F. Koster, Hantavirus fever without pulmonary syndrome in Panama, *Am. J. Trop. Med. Hyg.* 89 (2013) 489–494, <https://doi.org/10.4269/ajtmh.12-0334>.
- [23] D.H. Krüger, G. Schönrich, B. Klempa, Human pathogenic hantaviruses and prevention of infection, *Hum. Vaccine* 7 (2011) 685–693, <https://doi.org/10.4161/hv.7.6.15197>.
- [24] L. Zhang, Multi-epitope vaccines: a promising strategy against tumors and viral infections, *Cell. Mol. Immunol.* 15 (2018) 182–184, <https://doi.org/10.1038/cmi.2017.92>.
- [25] F. Abdulla, U.K. Adhikari, M.K. Uddin, Exploring T & B-cell epitopes and designing multi-epitope subunit vaccine targeting integration step of HIV-1 lifecycle using immunoinformatics approach, *Microb. Pathog.* 137 (2019) 103791, <https://doi.org/10.1016/j.micpath.2019.103791>.
- [26] M. Ali, R.K. Pandey, N. Khatoon, A. Narula, A. Mishra, V.K. Prajapati, Exploring dengue genome to construct a multi-epitope based subunit vaccine by utilizing immunoinformatics approach to battle against dengue infection, *Sci. Rep.* 7 (2017) 9232, <https://doi.org/10.1038/s41598-017-09199-w>.
- [27] E. Depla, A. Van der Aa, B.D. Livingston, C. Crimi, K. Allosery, V. De Brabandere, J. Krakover, S. Murthy, M. Huang, S. Power, L. Babé, C. Dahlberg, D. McKinney, A. Sette, S. Southwood, R. Philip, M.J. Newman, L. Meheus, Rational design of a multiepitope vaccine encoding T-lymphocyte epitopes for treatment of chronic hepatitis B virus infections, *J. Virol.* 82 (2008) 435–450, <https://doi.org/10.1128/JVI.01505-07>.
- [28] M. Nosrati, H. Mohabatkar, M. Behbahani, A novel multi-epitope vaccine for cross protection against hepatitis C virus (HCV): an immunoinformatics approach IT-, *Res-Mol-Med.* 5 (2017) 17–26, <https://doi.org/10.29252/rmm.5.1.17>.
- [29] A. Ikram, T. Zaheer, F.M. Awan, A. Obaid, A. Naz, R. Hanif, R.Z. Paracha, A. Ali, A.K. Naveed, H.A. Janjua, Exploring NS3/4A, NS5A and NS5B proteins to design conserved subunit multi-epitope vaccine against HCV utilizing immunoinformatics approaches, *Sci. Rep.* 8 (2018) 16107, <https://doi.org/10.1038/s41598-018-34254-5>.
- [30] S.I. Bazhan, D. V Antonots, L.I. Karpenko, S.F. Oreshkova, O.N. Kaplina, E. V Starostina, S.G. Dudko, S.A. Fedotova, A.A. Ilyichev, In silico designed Ebola virus T-cell multi-epitope DNA vaccine constructions are immunogenic in mice, *Vaccines* 7 (2019) 34, <https://doi.org/10.3390/vaccines7020034>.
- [31] A. Narula, R.K. Pandey, N. Khatoon, A. Mishra, V.K. Prajapati, Excavating chikungunya genome to design B and T cell multi-epitope subunit vaccine using comprehensive immunoinformatics approach to control chikungunya infection, *Infect. Genet. Evol.* 61 (2018) 4–15, <https://doi.org/10.1016/j.meegid.2018.03.007>.
- [32] M. Hasan, P.P. Ghosh, K.F. Azim, S. Mukta, R.A. Abir, J. Nahar, M.M. Hasan Khan, Reverse vaccinology approach to design a novel multi-epitope subunit vaccine against avian influenza A (H7N9) virus, *Microb. Pathog.* 130 (2019) 19–37, <https://doi.org/10.1016/j.micpath.2019.02.023>.
- [33] R. Kumar Pandey, R. Ojha, A. Mishra, V. Kumar Prajapati, Designing B- and T-cell multi-epitope based subunit vaccine using immunoinformatics approach to control Zika virus infection, *J. Cell. Biochem.* 119 (2018) 7631–7642, <https://doi.org/10.1002/jcb.27110>.
- [34] J. Ying, X. Dong, Y. Chen, Preliminary evaluation of a candidate multi-epitope-vaccine against the classical swine fever virus, *Tsinghua Sci. Technol.* 13 (2008) 433–438, [https://doi.org/10.1016/S1007-0214\(08\)70070-1](https://doi.org/10.1016/S1007-0214(08)70070-1).
- [35] R. Ojha, A. Pareek, R.K. Pandey, D. Prusty, V.K. Prajapati, Strategic development of a next-generation multi-epitope vaccine to prevent Nipah virus zoonotic infection, *ACS Omega* 4 (2019) 13069–13079, <https://doi.org/10.1021/acsomega.9b00944>.
- [36] K.F. Azim, M. Hasan, M.N. Hossain, S.R. Soman, S.F. Hoque, M.N.I. Bappy, A. T. Chowdhury, T. Lasker, Immunoinformatics approaches for designing a novel multi epitope peptide vaccine against human norovirus (Norwalk virus), *Infect. Genet. Evol.* 74 (2019) 103936, <https://doi.org/10.1016/j.meegid.2019.103936>.
- [37] D. Wang, J. Mai, W. Zhou, W. Yu, Y. Zhan, N. Wang, N.D. Epstein, Y. Yang, Immunoinformatic Analysis of T-And B-Cell Epitopes for SARS-CoV-2 Vaccine Design, *Vaccines*, 2020, <https://doi.org/10.3390/vaccines8030355>.
- [38] P. Kalita, A.K. Padhi, K.Y.J. Zhang, T. Tripathi, Design of a peptide-based subunit vaccine against novel coronavirus SARS-CoV-2, *Microb. Pathog.* (2020), <https://doi.org/10.1016/j.micpath.2020.104236>.
- [39] R. Liu, H. Ma, J. Shu, Q. Zhang, M. Han, Z. Liu, X. Jin, F. Zhang, X. Wu, Vaccines and therapeutics against hantaviruses, *Front. Microbiol.* 10 (2020) 2989, <https://doi.org/10.3389/fmicb.2019.02989>.
- [40] I.A. Doychinova, D.R. Flower, VaxiJen: a server for prediction of protective antigens, tumour antigens and subunit vaccines, *BMC Bioinf.* 8 (2007) 4, <https://doi.org/10.1186/1471-2105-8-4>.
- [41] M. V Larsen, C. Lundsgaard, K. Lamberth, S. Buus, O. Lund, M. Nielsen, Large-scale validation of methods for cytotoxic T-lymphocyte epitope prediction, *BMC Bioinf.* 8 (2007) 424, <https://doi.org/10.1186/1471-2105-8-424>.
- [42] M. Moutaftsi, B. Peters, V. Pasquetto, D.C. Tscharke, J. Sidney, H.-H. Bui, H. Grey, A. Sette, A consensus epitope prediction approach identifies the breadth of murine CD8+ cell responses to vaccinia virus, *Nat. Biotechnol.* 24 (2006) 817–819, <https://doi.org/10.1038/nbt1215>.
- [43] S.A. Kalams, S.P. Buchbinder, E.S. Rosenberg, J.M. Billingsley, D.S. Colbert, N. G. Jones, A.K. Shea, A.K. Trocha, B.D. Walker, Association between virus-specific cytotoxic T-lymphocyte and helper responses in human immunodeficiency virus type 1 infection, *J. Virol.* (1999), <https://doi.org/10.1128/jvi.73.8.6715-6720.1999>.

- [44] D.S. Rosa, S.P. Ribeiro, E. Cunha-Neto, CD4+ T cell epitope discovery and rational vaccine design, *Arch. Immunol. Ther. Exp.* (2010), <https://doi.org/10.1007/s00005-010-0067-0>.
- [45] P. Wang, J. Sidney, Y. Kim, A. Sette, O. Lund, M. Nielsen, B. Peters, Peptide binding predictions for HLA DR, DP and DQ molecules, *BMC Bioinf.* 11 (2010) 568, <https://doi.org/10.1186/1471-2105-11-568>.
- [46] M.C. Jespersen, B. Peters, M. Nielsen, P. Marcattili, BepiPred-2.0: improving sequence-based B-cell epitope prediction using conformational epitopes, *Nucleic Acids Res.* 45 (2017) W24–W29, <https://doi.org/10.1093/nar/gkx346>.
- [47] H. Singh, H.R. Ansari, G.P.S. Raghava, Improved method for linear B-cell epitope prediction using antigen's primary sequence, *PLoS One* 8 (2013), e62216, <https://doi.org/10.1371/journal.pone.0062216>.
- [48] G. Leroux-Roels, P. Bonanni, T. Tantawichien, F. Zepp, Vaccine development, perspectives in vaccinology, 1, 2011, pp. 115–150, <https://doi.org/10.1016/j.pervac.2011.05.005>.
- [49] J.J.A. Calis, M. Maybeno, J.A. Greenbaum, D. Weiskopf, A.D. De Silva, A. Sette, C. Keşmir, B. Peters, Properties of MHC class I presented peptides that enhance immunogenicity, *PLoS Comput. Biol.* 9 (2013), e1003266, <https://doi.org/10.1371/journal.pcbi.1003266> e1003266.
- [50] H.-H. Bui, J. Sidney, W. Li, N. Fusseder, A. Sette, Development of an epitope conservancy analysis tool to facilitate the design of epitope-based diagnostics and vaccines, *BMC Bioinf.* 8 (2007) 361, <https://doi.org/10.1186/1471-2105-8-361>.
- [51] I. Dimitrov, D.R. Flower, I. Doytchinova, AllerTOP-a server for in silico prediction of allergens, *BMC Bioinf.* 14 (Suppl 6) (2013) S4, [https://doi.org/10.1186/1471-2105-14-S4\\_S4](https://doi.org/10.1186/1471-2105-14-S4_S4).
- [52] S. Gupta, P. Kapoor, K. Chaudhary, A. Gautam, R. Kumar, O.S.D.D. Consortium, G.P.S. Raghava, In silico approach for predicting toxicity of peptides and proteins, *PLoS One* 8 (2013), e73957, <https://doi.org/10.1371/journal.pone.0073957>.
- [53] H.-H. Bui, J. Sidney, K. Dinh, S. Southwood, M.J. Newman, A. Sette, Predicting population coverage of T-cell epitope-based diagnostics and vaccines, *BMC Bioinf.* 7 (2006) 153, <https://doi.org/10.1186/1471-2105-7-153>.
- [54] M. Linderholm, C. Ahlm, B. Settergren, A. Waage, A. Tärnvik, Elevated plasma levels of tumor necrosis factor (TNF)- $\alpha$ , soluble TNF receptors, interleukin (IL)-6, and IL-10 in patients with hemorrhagic fever with renal syndrome, *J. Infect. Dis.* 173 (1996) 38–43, <https://doi.org/10.1093/infdis/173.1.38>.
- [55] T.K. Outinen, S.M. Mäkelä, I.O. Ala-Houhala, H.S.A. Huhtala, M. Hurme, A. S. Paakkala, I.H. Pörsti, J.T. Syrjänen, J.T. Mustonen, The severity of Puumala hantavirus induced nephropathia epidemica can be better evaluated using plasma interleukin-6 than C-reactive protein determinations, *BMC Infect. Dis.* 10 (2010) 132, <https://doi.org/10.1186/1471-2334-10-132>.
- [56] H. Jiang, P.-Z. Wang, Y. Zhang, Z. Xu, L. Sun, L.-M. Wang, C.-X. Huang, J.-Q. Lian, Z.-S. Jia, Z.-D. Li, X.-F. Bai, Hantaan virus induces toll-like receptor 4 expression, leading to enhanced production of beta interferon, interleukin-6 and tumor necrosis factor-alpha, *Virology* 380 (2008) 52–59, <https://doi.org/10.1016/j.virol.2008.07.002>.
- [57] M. Niikura, A. Maeda, T. Ikegami, M. Sajio, I. Kurane, S. Morikawa, Modification of endothelial cell functions by Hantaan virus infection: prolonged hyperpermeability induced by TNF-alpha of Hantaan virus-infected endothelial cell monolayers, *Arch. Virol.* 149 (2004) 1279–1292, <https://doi.org/10.1007/s00705-004-0306-y>.
- [58] M. Terajima, D. Hayasaka, K. Maeda, F.A. Ennis, Immunopathogenesis of hantavirus pulmonary syndrome and hemorrhagic fever with renal syndrome: do CD8+ T cells trigger capillary leakage in viral hemorrhagic fevers? *Immunol. Lett.* 113 (2007) 117–120, <https://doi.org/10.1016/j.imlet.2007.08.003>.
- [59] G. Nagpal, S.S. Usmani, S.K. Dhandha, H. Kaur, S. Singh, M. Sharma, G.P. S. Raghava, Computer-aided designing of immunosuppressive peptides based on IL-10 inducing potential, *Sci. Rep.* 7 (2017) 42851, <https://doi.org/10.1038/srep42851>.
- [60] G.M. Morris, M. Lim-Wilby, in: A. Kukol (Ed.), *Molecular Docking BT - Molecular Modeling of Proteins*, Humana Press, Totowa, NJ, 2008, pp. 365–382, [https://doi.org/10.1007/978-1-5945-177-2\\_19](https://doi.org/10.1007/978-1-5945-177-2_19).
- [61] A. Lamiable, P. Thévenet, J. Rey, M. Vavrusa, P. Derreumaux, P. Tufféry, PEP-FOLD3: faster de novo structure prediction for linear peptides in solution and in complex, *Nucleic Acids Res.* 44 (2016) W449–W454, <https://doi.org/10.1093/nar/gkw329>.
- [62] K.F. Chan, B.S. Gully, S. Gras, D.X. Beringer, L. Kjer-Nielsen, J. Cebon, J. McCluskey, W. Chen, J. Rossjohn, Divergent T-cell receptor recognition modes of a HLA-I restricted extended tumour-associated peptide, *Nat. Commun.* 9 (2018) 1026, <https://doi.org/10.1038/s41467-018-03321-w>.
- [63] R.M. McMahon, L. Friis, C. Siebold, M.A. Fries, L. Fugger, E.Y. Jones, Structure of HLA-A\*0301 in complex with a peptide of proteolipid protein: insights into the role of HLA-A alleles in susceptibility to multiple sclerosis, *Acta Crystallographica. Section D, Biological Crystallography* 67 (2011) 447–454, <https://doi.org/10.1107/S0907444911007888>.
- [64] A. Culshaw, K. Ladell, S. Gras, J.E. McLaren, K.L. Miners, C. Farenc, H. van den Heuvel, E. Gostick, W. Dejnirattisai, A. Wangteeraprasert, T. Duangchinda, P. Chotiyarnwong, W. Limpitikul, S. Vasanawathana, P. Malasit, T. Dong, J. Rossjohn, J. Mongkolsapaya, D.A. Price, G.R. Scream, Germline bias dictates cross-serotype reactivity in a common dengue-virus-specific CD8+ T cell response, *Nat. Immunol.* 18 (2017) 1228, <https://doi.org/10.1038/ni.3850>.
- [65] J.I. Mobbs, P.T. Illing, N.L. Dudek, A.G. Brooks, D.G. Baker, A.W. Purcell, J. Rossjohn, J.P. Vivian, The molecular basis for peptide repertoire selection in the human leucocyte antigen (HLA) C\*06:02 molecule, *J. Biol. Chem.* 292 (2017) 17203–17215, <https://doi.org/10.1074/jbc.M117.806976>.
- [66] K. Maenaka, T. Maenaka, H. Tomiyama, M. Takiguchi, D.I. Stuart, E.Y. Jones, Nonstandard peptide binding revealed by crystal structures of HLA-B\*5101 complexed with HIV immunodominant epitopes, *J. Immunol.* 165 (2000) 3260–3267, <https://doi.org/10.4049/jimmunol.165.3.3260>.
- [67] M. Sun, J. Liu, J. Qi, B. Tefsen, Y. Shi, J. Yan, G.F. Gao, N-terminal acetylation for T cell recognition: molecular basis of MHC class I-restricted  $\alpha\alpha$ -acetylpeptide presentation, *J. Immunol.* 192 (2014) 5509–5519, <https://doi.org/10.4049/jimmunol.1400199>.
- [68] J. Liu, S. Zhang, S. Tan, Y. Yi, B. Wu, B. Cao, F. Zhu, C. Wang, H. Wang, J. Qi, G. F. Gao, Cross-allele cytotoxic T lymphocyte responses against 2009 pandemic H1N1 influenza A virus among HLA-A24 and HLA-A3 supertype-positive individuals, *J. Virol.* 86 (2012) 13281–13294, <https://doi.org/10.1128/JVI.01841-12>.
- [69] A. Alpizar, M. Marcilla, C. Santiago, Structure of HLA-B\*40:02 in Complex with the Endogenous Peptide REFSKEPEL, TO BE PUBLISHED. (n.d.). doi:10.2210/PDB5IEK/PDB.
- [70] E.J. Grant, T.M. Josephs, L. Loh, E.B. Clemens, S. Sant, M. Bharadwaj, W. Chen, J. Rossjohn, S. Gras, K. Kedzierska, Broad CD8+ T cell cross-recognition of distinct influenza A strains in humans, *Nat. Commun.* 9 (2018) 5427, <https://doi.org/10.1038/s41467-018-07815-5>.
- [71] E.F. Rosloniec, R.A. Ivey, K.B. Whittington, A.H. Kang, H.-W. Park, Crystallographic structure of a rheumatoid arthritis MHC susceptibility allele, <em>HLA-DR1</em> (<em>DRB1\*0101</em>), complexed with the immunodominant determinant of human type II collagen, *J. Immunol.* 177 (2006) 3884–3892, <https://doi.org/10.4049/jimmunol.177.6.3884>.
- [72] G.M. Morris, R. Huey, W. Lindstrom, M.F. Sanner, R.K. Belew, D.S. Goodsell, A. J. Olson, AutoDock4 and AutoDockTools4: automated docking with selective receptor flexibility, *J. Comput. Chem.* 30 (2009) 2785–2791, <https://doi.org/10.1002/jcc.21256>.
- [73] O. Trott, A.J. Olson, AutoDock Vina, Improving the speed and accuracy of docking with a new scoring function, efficient optimization, and multithreading, *J. Comput. Chem.* 31 (2010) 455–461, <https://doi.org/10.1002/jcc.21334>.
- [74] J.C. Tong, T.W. Tan, S. Ranganathan, in: R.K. De, N. Tomar (Eds.), *Structure-Based Clustering of Major Histocompatibility Complex (MHC) Proteins for Broad-Based T-Cell Vaccine Design BT - Immunoinformatics*, Springer New York, New York, NY, 2014, pp. 503–511, [https://doi.org/10.1007/978-1-4939-1115-8\\_27](https://doi.org/10.1007/978-1-4939-1115-8_27).
- [75] M. Thomsen, C. Lundsgaard, S. Buus, O. Lund, M. Nielsen, MHCcluster, a method for functional clustering of MHC molecules, *Immunogenetics* 65 (2013) 655–665, <https://doi.org/10.1007/s00251-013-0714-9>.
- [76] N. Nezafat, Y. Ghasemi, G. Javadi, M.J. Khoshnoud, E. Omidinia, A novel multi-epitope peptide vaccine against cancer: an in silico approach, *J. Theor. Biol.* 349 (2014) 121–134, <https://doi.org/10.1016/j.jtbi.2014.01.018>.
- [77] N. Rahman, F. Ali, Z. Basharat, M. Shehroz, M.K. Khan, P. Jeandet, E. Nepomivova, K. Kuca, H. Khan, Vaccine design from the ensemble of surface glycoprotein epitopes of SARS-CoV-2: an immunoinformatics approach, *Vaccines* 8 (2020) 1–17, <https://doi.org/10.3390/vaccines8030423>.
- [78] N. Khatoon, R.K. Pandey, V.K. Prajapati, Exploring Leishmania secretory proteins to design B and T cell multi-epitope subunit vaccine using immunoinformatics approach, *Sci. Rep.* 7 (2017) 8285, <https://doi.org/10.1038/s41598-017-08842-w>.
- [79] R.K. Pandey, R. Ojha, V.S. Aathmanathan, M. Krishnan, V.K. Prajapati, Immunoinformatics approaches to design a novel multi-epitope subunit vaccine against HIV infection, *Vaccine* 36 (2018) 2262–2272, <https://doi.org/10.1016/j.vaccine.2018.03.042>.
- [80] R.K. Pandey, T.K. Bhatt, V.K. Prajapati, Novel immunoinformatics approaches to design multi-epitope subunit vaccine for malaria by investigating Anopheles salivary protein, *Sci. Rep.* 8 (2018) 1125, <https://doi.org/10.1038/s41598-018-19456-1>.
- [81] S. Saha, G.P.S. Raghava, AlgPred: prediction of allergenic proteins and mapping of IgE epitopes, *Nucleic Acids Res.* 34 (2006) W202–W209, <https://doi.org/10.1093/nar/gkl343>.
- [82] I. Dimitrov, L. Naneva, I. Doytchinova, I. Bangov, AllergenFP: allergenicity prediction by descriptor fingerprints, *Bioinformatics* 30 (2013) 846–851, <https://doi.org/10.1093/bioinformatics/btt619>.
- [83] C. Geourjon, G. Deléage, SOPMA: significant improvements in protein secondary structure prediction by consensus prediction from multiple alignments, *Bioinformatics* 11 (1995) 681–684, <https://doi.org/10.1093/bioinformatics/11.6.681>.
- [84] M. Källberg, H. Wang, S. Wang, J. Peng, Z. Wang, H. Lu, J. Xu, Template-based protein structure modeling using the RaptorX web server, *Nat. Protoc.* 7 (2012) 1511–1522, <https://doi.org/10.1038/nprot.2012.085>.
- [85] R. Adiyaman, L.J. McGuffin, Methods for the refinement of protein structure 3D models, *Int. J. Mol. Sci.* 20 (2019) 2301, <https://doi.org/10.3390/ijms20092301>.
- [86] L. Heo, H. Park, C. Seok, GalaxyRefine: protein structure refinement driven by side-chain repacking, *Nucleic Acids Res.* 41 (2013) W384–W388, <https://doi.org/10.1093/nar/gkt458>.
- [87] R.A. Laskowski, M.W. MacArthur, D.S. Moss, J.M. Thornton, PROCHECK: a program to check the stereochemical quality of protein structures, *J. Appl. Crystallogr.* 26 (1993) 283–291, <https://doi.org/10.1107/S0021889892009944>.
- [88] R.A. Laskowski, J. Jablonska, L. Pravda, R.S. Varekova, J.M. Thornton, PDBsum: structural summaries of PDB entries, *Protein Science, A Publication of the Protein Society* 27 (2018) 129–134, <https://doi.org/10.1002/pro.3289>.
- [89] M. Wiederstein, M.J. Sippl, ProSA-web: interactive web service for the recognition of errors in three-dimensional structures of proteins, *Nucleic Acids Res.* 35 (2007) W407–W410, <https://doi.org/10.1093/nar/gkm290>.
- [90] C. Colovos, T.O. Yeates, Verification of protein structures: patterns of nonbonded atomic interactions, *Protein Science, A Publication of the Protein Society* 2 (1993) 1511–1519, <https://doi.org/10.1002/pro.5560020916>.

- [91] M.R. Wilkins, E. Gasteiger, A. Bairoch, J.-C. Sanchez, K.L. Williams, R.D. Appel, D.F. Hochstrasser, in: A.J. Link (Ed.), Protein Identification and Analysis Tools in the ExPASy Server BT - 2-D Proteome Analysis Protocols, Humana Press, Totowa, NJ, 1999, pp. 531–552, <https://doi.org/10.1385/1-59259-584-7:531>.
- [92] C.N. Magnan, A. Randall, P. Baldi, SOLpro: accurate sequence-based prediction of protein solubility, *Bioinformatics* 25 (2009) 2200–2207, <https://doi.org/10.1093/bioinformatics/btp386>.
- [93] J. Ponomarenko, H.-H. Bui, W. Li, N. Fusseder, P.E. Bourne, A. Sette, B. Peters, ElliPro: a new structure-based tool for the prediction of antibody epitopes, *BMC Bioinf.* 9 (2008) 514, <https://doi.org/10.1186/1471-2105-9-514>.
- [94] D.B. Craig, A.A. Dombrowski, Disulfide by Design 2.0: a web-based tool for disulfide engineering in proteins, *BMC Bioinf.* 14 (2013) 346, <https://doi.org/10.1186/1471-2105-14-346>.
- [95] C.H.M. Rodrigues, D.E. Vpires, D.B. Ascher, DynaMut: predicting the impact of mutations on protein conformation, flexibility and stability, *Nucleic Acids Res.* 46 (2018) W350–W355, <https://doi.org/10.1093/nar/gky300>.
- [96] X.-Y. Meng, H.-X. Zhang, M. Mezei, M. Cui, Molecular docking: a powerful approach for structure-based drug discovery, *Curr. Comput. Aided Drug Des.* 7 (2011) 146–157, <https://www.ncbi.nlm.nih.gov/pubmed/21534921>.
- [97] H.-T. Yu, H. Jiang, Y. Zhang, X.-P. Nan, Y. Li, W. Wang, W. Jiang, D.-Q. Yang, W.-J. Su, J.-P. Wang, P.-Z. Wang, X.-F. Bai, Hantavirus triggers TLR4-dependent innate immune responses, *Viral Immunol.* 25 (2012) 387–393, <https://doi.org/10.1089/vim.2012.0005>.
- [98] D. Kozakov, D.R. Hall, B. Xia, K.A. Porter, D. Padhorny, C. Yueh, D. Beglov, S. Vajda, The ClusPro web server for protein–protein docking, *Nat. Protoc.* 12 (2017) 255, <https://doi.org/10.1038/nprot.2016.169>.
- [99] D. Duhovny, R. Nussinov, H.J. Wolfson, Efficient unbound docking of rigid molecules, *Lect. Notes Comput. Sci.* 2452 (2002) 185–200, [https://doi.org/10.1007/3-540-45784-4\\_14](https://doi.org/10.1007/3-540-45784-4_14).
- [100] D. Schneidman-Duhovny, Y. Inbar, R. Nussinov, H.J. Wolfson, PatchDock and SymmDock: servers for rigid and symmetric docking, *Nucleic Acids Res.* 33 (2005) 363–367, <https://doi.org/10.1093/nar/gki481>.
- [101] N. Andrusier, R. Nussinov, H.J. Wolfson, FireDock: fast interaction refinement in molecular docking, *Proteins: Structure, Function, and Bioinformatics* 69 (2007) 139–159, <https://doi.org/10.1002/prot.21495>.
- [102] E. Mashiafach, D. Schneidman-Duhovny, N. Andrusier, R. Nussinov, H.J. Wolfson, FireDock: a web server for fast interaction refinement in molecular docking †, *Nucleic Acids Res.* 36 (2008) W229–W232, <https://doi.org/10.1093/nar/gkn186>.
- [103] M. Karplus, J.A. McCammon, Molecular dynamics simulations of biomolecules, *Nat. Struct. Biol.* 9 (2002) 646–652, <https://doi.org/10.1038/nsb0902-646>.
- [104] J.R. López-Blanco, J.I. Garzón, P. Chacón, iMod: multipurpose normal mode analysis in internal coordinates, *Bioinformatics* 27 (2011) 2843–2850, <https://doi.org/10.1093/bioinformatics/btr497>.
- [105] F. Tama, C.L. Brooks, SYMMETRY, form, and shape: guiding principles for robustness in macromolecular machines, *Annu. Rev. Biophys. Biomol. Struct.* 35 (2006) 115–133, <https://doi.org/10.1146/annurev.biophys.35.040405.102010>.
- [106] S. Meroueh, Normal mode analysis theoretical and applications to biological and chemical systems, *Briefings Bioinf.* 8 (2007) 378–379, <https://doi.org/10.1093/bib/bbm010>.
- [107] J.R. López-Blanco, J.I. Aliaga, E.S. Quintana-Ortí, P. Chacón, iMODS: internal coordinates normal mode analysis server, *Nucleic Acids Res.* 42 (2014) W271–W276, <https://doi.org/10.1093/nar/gku339>.
- [108] A. Grote, K. Hiller, M. Scheer, R. Münnich, B. Nörtemann, D.C. Hempel, D. Jahn, JCat: a novel tool to adapt codon usage of a target gene to its potential expression host, *Nucleic Acids Res.* 33 (2005) W526–W531, <https://doi.org/10.1093/nar/gki376>.
- [109] N. Rapin, O. Lund, M. Bernaschi, F. Castiglione, Computational immunology meets bioinformatics: the use of prediction tools for molecular binding in the simulation of the immune system, *PLoS One* 5 (2010), e9862, <https://doi.org/10.1371/journal.pone.0009862>.
- [110] F. Castiglione, F. Mantile, P. De Berardinis, A. Prisco, How the interval between prime and boost injection affects the immune response in a computational model of the immune system, *Computational and Mathematical Methods in Medicine* (2012) 842329, <https://doi.org/10.1155/2012/842329>, 2012.
- [111] R.A. Shey, S.M. Ghogomu, K.K. Esoh, N.D. Nebangwa, C.M. Shintouo, N. Fongley, B.F. Asa, F.N. Ngale, L. Vanhamme, J. Souopgui, In-silico design of a multi-epitope vaccine candidate against onchocerciasis and related filarial diseases, *Sci. Rep.* 9 (2019) 4409, <https://doi.org/10.1038/s41598-019-40833-x>.
- [112] M. Sadeghi, I. Eckerle, V. Daniel, U. Burkhardt, G. Opelz, P. Schnitzler, Cytokine expression during early and late phase of acute Puumala hantavirus infection, *BMC Immunol.* 12 (2011) 65, <https://doi.org/10.1186/1471-2172-12-65>.
- [113] U.K. Adhikari, M.M. Rahman, Overlapping CD8+ and CD4+ T-cell epitopes identification for the progression of epitope-based peptide vaccine from nucleocapsid and glycoprotein of emerging Rift Valley fever virus using immunoinformatics approach, *Infect. Genet. Evol.* 56 (2017) 75–91, <https://doi.org/10.1016/j.meegid.2017.10.022>.
- [114] U.K. Adhikari, M. Tayebi, M.M. Rahman, Immunoinformatics approach for epitope-based peptide vaccine design and active site prediction against polyprotein of emerging oropouche virus, *Journal of Immunology Research* (2018) 6718083, <https://doi.org/10.1155/2018/6718083>, 2018.
- [115] H.W. Lee, P.W. Lee, K.M. Johnson, Isolation of the etiologic agent of Korean hemorrhagic fever, *J. Infect. Dis.* 137 (1978) 298–308, <https://doi.org/10.1093/infdis/137.3.298>.
- [116] J. Latus, M. Schwab, E. Tacconelli, F.-M. Pieper, D. Wegener, B. Rettenmaier, A. Schwab, L. Hoffmann, J. Dippon, S. Müller, P. Fritz, D. Zakim, S. Segerer, D. Kitterer, M. Kimmel, K. Gußmann, M. Priwitzer, B. Mezger, B. Walter-Frank, A. Corea, A. Wiedenmann, S. Brockmann, C. Pöhlmann, M.D. Alscher, N. Braun, Acute kidney injury and tools for risk-stratification in 456 patients with hantavirus-induced nephropathia epidemica, *Nephrol. Dial. Transplant.* 30 (2014) 245–251, <https://doi.org/10.1093/ndt/gfu319>.
- [117] M. Brummer-Korvenkontio, A. Vaheri, T. Hovi, C.-H. von Bonsdorff, J. Vuorimies, T. Manni, K. Penttilinen, N. Oker-Blom, J. Lähdevirta, Nephropathia Epidemica, Detection of antigen in bank voles and serologic diagnosis of human infection, *J. Infect. Dis.* 141 (1980) 131–134, <https://doi.org/10.1093/infdis/141.2.131>.
- [118] P. Vollmar, M. Lubnow, M. Simon, T. Müller, T. Bergler, P. Alois, B.R. Thoma, S. Essbauer, Hantavirus cardiopulmonary syndrome due to Puumala virus in Germany, *J. Clin. Virol.* 84 (2016) 42–47, <https://doi.org/10.1016/j.jcv.2016.10.004>.
- [119] J.Y. Noh, H.J. Cheong, J.Y. Song, W.J. Kim, K.-J. Song, T.A. Klein, S.H. Lee, R. Yanagihara, J.-W. Song, Clinical and molecular epidemiological features of hemorrhagic fever with renal syndrome in Korea over a 10-year period, *J. Clin. Virol.* 58 (2013) 11–17, <https://doi.org/10.1016/j.jcv.2013.06.027>.
- [120] L.-S. Yao, C.-F. Qin, Y. Pu, X.-L. Zhang, Y.-X. Liu, Y. Liu, X. Cao, Y.-Q. Deng, J. Wang, K.-X. Hu, B.-L. Xu, Complete genome sequence of Seoul virus isolated from Rattus norvegicus in the Democratic People's Republic of Korea, *J. Virol.* 86 (2012) 13853, <https://doi.org/10.1128/JVI.02668-12>.
- [121] A. Papa, Dobrava-Belgrade virus: phylogeny, epidemiology, disease, *Antivir. Res.* 95 (2012) 104–117, <https://doi.org/10.1016/j.antiviral.2012.05.011>.
- [122] V. Nikolic, N. Stajkovic, G. Stamenkovic, R. Cekanac, P. Mariusic, M. Siljic, A. Gligic, M. Stanjevic, Evidence of recombination in Tula virus strains from Serbia, *Infect. Genet. Evol.* 21 (2014) 472–478, <https://doi.org/10.1016/j.mee.2013.08.020>.
- [123] S. Pattamadilok, B.-H. Lee, S. Kumperasart, K. Yoshimatsu, M. Okumura, I. Nakamura, K. Araki, Y. Khoprasert, P. Dangsupa, P. Panlar, B. Jandrig, D. H. Krüger, B. Klempa, T. Jäkel, J. Schmidt, R. Ulrich, H. Kariwa, J. Arikawa, Geographical distribution OF hantaviruses IN Thailand and potential human health significance OF Thailand virus, *Am. J. Trop. Med. Hyg.* 75 (2006) 994–1002, <https://doi.org/10.4269/ajtmh.2006.75.994>.
- [124] C.D. Gamage, S.P. Yasuda, S. Nishio, S.A. Kularatne, K. Weerakoon, J. Rajapakse, C. Nwafor-Okoli, R.B. Lee, Y. Obayashi, K. Yoshimatsu, J. Arikawa, H. Tamashiro, Serological evidence of Thailand virus-related hantavirus infection among suspected leptospirosis patients in Kandy, Sri Lanka, *Jpn. J. Infect. Dis.* 64 (2011) 72–75.
- [125] V. Raharinosy, M.-M. Olive, F.M. Andriamiarimanana, S.F. Andriamandimbry, J.-P. Ravalohery, S. Andriamamonjy, C. Filippone, D.A.D. Rakoto, S. Telfer, J.-M. Heraud, Geographical distribution and relative risk of Anjozorobe virus (Thailand orthohantavirus) infection in black rats (*Rattus rattus*) in Madagascar, *Virol. J.* 15 (2018) 83, <https://doi.org/10.1186/s12985-018-0992-9>.
- [126] B. Klempa, L. Koivogui, O. Sylla, K. Koulemou, B. Auste, D.H. Krüger, J. ter Meulen, Serological evidence of human hantavirus infections in Guinea, West Africa, *J. Infect. Dis.* 201 (2010) 1031–1034, <https://doi.org/10.1086/651169>.
- [127] T.G. Ksiazek, C.J. Peters, P.E. Rollin, S. Zaki, S. Nichol, C. Spiropoulou, S. Morzunov, H. Feldmann, A. Sanchez, A.S. Khan, B.W.J. Mahy, K. Wachsmuth, J.C. Butler, Identification of a new North American hantavirus that causes acute pulmonary insufficiency, *Am. J. Trop. Med. Hyg.* 52 (1995) 117–123, <https://doi.org/10.4269/ajtmh.1995.52.1.117>.
- [128] T. Avšič-Županc, A. Saksida, M. Korva, Hantavirus infections, *Clin. Microbiol. Infect.* 21 (2019) e6–e16, <https://doi.org/10.1111/1469-0691.12291>.
- [129] S.L. Hinrichsen, J.T. Godoi, Hantavirus disease, *Rev. Assoc. Méd. Bras.* 42 (1996) (1992) 237–241.
- [130] C.H. Calisher, J.J. Root, J.N. Mills, J.E. Rowe, S.A. Reeder, E.S. Jentes, K. Wagoner, B.J. Beaty, Epizootiology OF SIN nombre and el moro canyon hantaviruses, southeastern Colorado, 1995–2000, *J. Wildl. Dis.* 41 (2005) 1–11, <https://doi.org/10.7589/0090-3558-41.1.1>.
- [131] A. Rahmani, M. Baez, M. Rostamtabar, A. Karkhah, S. Alizadeh, M. Tourani, H. R. Nouri, Development of a conserved chimeric vaccine based on helper T-cell and CTL epitopes for induction of strong immune response against *Schistosoma mansoni* using immunoinformatics approaches, *Int. J. Biol. Macromol.* 141 (2019) 125–136, <https://doi.org/10.1016/j.ijbiomac.2019.08.259>.
- [132] P. Kalita, D.L. Lyngdoh, A.K. Padhi, H. Shukla, T. Tripathi, Development of multi-epitope driven subunit vaccine against *Fasciola gigantica* using immunoinformatics approach, *Int. J. Biol. Macromol.* 138 (2019) 224–233, <https://doi.org/10.1016/j.ijbiomac.2019.07.024>.
- [133] A. Shanmugam, S. Rajoria, A.L. George, A. Mittelman, R. Suriano, R.K. Tiwari, Synthetic toll like receptor-4 (TLR-4) agonist peptides as a novel class of adjuvants, *PLoS One* 7 (2012), e30839, <https://doi.org/10.1371/journal.pone.0030839>.
- [134] T. Mohan, C. Sharma, A.A. Bhat, D.N. Rao, Modulation of HIV peptide antigen specific cellular immune response by synthetic α- and β-defensin peptides, *Vaccine* 31 (2013) 1707–1716, <https://doi.org/10.1016/j.vaccine.2013.01.041>.
- [135] S.J. Lee, S.J. Shin, M.H. Lee, M.-G. Lee, T.H. Kang, W.S. Park, B.Y. Soh, J.H. Park, Y.K. Shin, H.W. Kim, C.-H. Yun, I.D. Jung, Y.-M. Park, A potential protein adjuvant derived from *Mycobacterium tuberculosis* Rv0652 enhances dendritic cells-based tumor immunotherapy, *PloS One* 9 (2014), e104351, <https://doi.org/10.1371/journal.pone.0104351>.
- [136] S. Deshayes, M. Morris, G. Divita, F. Heitz, Cell-penetrating peptides: tools for intracellular delivery of therapeutics, *Cell. Mol. Life Sci.: CMLS* 62 (2005) 1839–1849, <https://doi.org/10.1007/s0018-005-5109-0>.
- [137] K. Kardani, A. Milani, S.H. Shabani, A. Bolhassani, Cell penetrating peptides: the potent multi-cargo intracellular carriers, *Expert Opin. Drug Deliv.* 16 (2019) 1227–1258, <https://doi.org/10.1080/17425247.2019.1676720>.

- [138] J. Váňová, A. Hejtmánková, M.H. Kalbáčová, H. Španielová, The utilization of cell-penetrating peptides in the intracellular delivery of viral nanoparticles, *Materials* 12 (2019) 2671, <https://doi.org/10.3390/ma12172671>.
- [139] J. Yang, Y. Luo, M.A. Shibu, I. Toth, M. Skwarczynska, Cell-penetrating peptides: efficient vectors for vaccine delivery, *Curr. Drug Deliv.* 16 (2019) 430–443, <https://doi.org/10.2174/1567201816666190123120915>.
- [140] A. Naz, F.M. Awan, A. Obaid, S.A. Muhammad, R.Z. Paracha, J. Ahmad, A. Ali, Identification of putative vaccine candidates against *Helicobacter pylori* exploiting exoproteome and secretome: a reverse vaccinology based approach, *Infect. Genet. Evol.* 32 (2015) 280–291, <https://doi.org/10.1016/j.meegid.2015.03.027>.
- [141] J.A. Kovacs, P. Chacón, R. Abagyan, Predictions of protein flexibility: first-order measures, *Proteins: Structure, Function, and Bioinformatics* 56 (2004) 661–668, <https://doi.org/10.1002/prot.20151>.
- [142] T. Ichijo, M. Karplus, Collective motions in proteins: a covariance analysis of atomic fluctuations in molecular dynamics and normal mode simulations, *Proteins: Structure, Function, and Bioinformatics* 11 (1991) 205–217, <https://doi.org/10.1002/prot.340110305>.
- [143] M.S. Duthie, H.P. Windish, C.B. Fox, S.G. Reed, Use of defined TLR ligands as adjuvants within human vaccines, *Immunol. Rev.* 239 (2011) 178–196, <https://doi.org/10.1111/j.1600-065X.2010.00978.x>.